Dual Craig-Bampton Component Mode Synthesis Method for Model Order Reduction of Nonclassically Damped Linear Systems

Fabian M. Gruber*, Daniel J. Rixen

Technical University of Munich, Faculty of Mechanical Engineering, Institute of Applied Mechanics, Boltzmannstr. 15, 85748 Garching, Germany

Abstract

The original dual Craig-Bampton method for reducing and successively coupling undamped substructured systems is extended to the case of arbitrary viscous damping.

The reduction is based on the equations of motion in state-space representation and uses complex free interface normal modes, residual flexibility modes, and state-space rigid body modes. To couple the substructures in state-space representation, a dual coupling procedure based on the interface forces between adjacent substructures is used, which is novel compared to other methods commonly applying primal coupling procedures in state-space representation.

The very good approximation accuracy for arbitrary viscous damping of the dual Craig-Bampton approach is demonstrated on a beam structure with localized dampers. The results are compared to a classical Craig-Bampton approach for damped systems showing the potential of the proposed method.

Keywords: Model order reduction, Component mode synthesis, Dynamic substructuring, Dual Craig-Bampton method, Nonclassically damped systems, State-space formulation, Complex modes

1. Introduction

The increasing performance of modern computers makes it possible to solve very large linear systems of millions of degrees of freedom (DOFs) very fast. Since the refinement of finite element models is increasing faster than the computing capabilities, dynamic substructuring techniques or component mode synthesis methods still remain an essential tool for analyzing dynamical systems in an efficient manner. Componentwise analysis and building reduced models of submodels of structures has important advantages over global methods where the entire structure is handled at once. The dynamic behavior of structures that are too large to be analyzed as a whole can be evaluated. For finite element models, dynamic substructuring provides fast solutions when the number of DOFs is so large that solutions can not be found in a reasonable time for the global structure. Furthermore, building reduced models of submodels of a structure enables sharing models between design groups and also combining models from different project groups. Thereby, each group does not have to disclose the detailed model that was used for the design. Only a reduced model of the component, which was engineered by one group, has to be shared with the other design groups or companies. Significantly less memory storage has to be used if reduced models including only necessary information are saved and shared. Moreover, the reduction of the DOFs of substructures is also important for building reduced-order models for optimization and control. Controllers can typically be designed only for models up to a small number of DOFs. Most optimization procedures perform many iterations for certain parameters of a model, which is much faster and more efficient if reduced models can be used. If a single component of a system is changed or optimized, only that component needs to be reanalyzed/reoptimized

---

*Corresponding author

Email addresses: `fabian.gruber@tum.de` (Fabian M. Gruber), `rixen@tum.de` (Daniel J. Rixen)

and the entire assembled system can be analyzed at low additional cost. Thus, dynamic substructuring offers a very flexible approach to dynamic analysis [1, 2, 3, 4, 5, 6, 7, 8].

Dynamic substructuring techniques reduce the size of large models. The large model is thereby divided into N substructures; each substructure is analyzed and reduced separately and then assembled into a low-order reduced model. This low-order reduced model approximates the original large model's behavior. During this process, each substructure's DOFs are commonly divided into internal DOFs (those not shared with any adjacent substructure) and boundary or interface DOFs (those shared with adjacent substructures and therefore forming the model's interface DOFs). Many substructuring methods that work with second-order equations of motion have been proposed in the past [1, 2, 3, 5, 9, 10, 11]. Only the substructures' mass and stiffness properties are commonly taken into account for the reduction. In doing so, the undamped equations of motion are assumed to correctly describe the substructure dynamics and it is assumed that there is no damping or that damping effects are completely negligible when building the reduction basis. Most substructuring methods work with the undamped equations of motion and afford great approximation accuracy if the underlying system is damped only slightly or not at all.

Dynamic substructuring techniques can be classified depending on the underlying modes that are used [4]. The term mode can refer to all kinds of structural shape vectors. The most popular approach is a fixed interface method, the Craig-Bampton method [1], which is based on fixed interface normal modes and interface constraint modes. The substructures are assembled using interface displacements, which is referred to as primal assembly. Many other methods, such as those of MacNeal [2], Rubin [3], and Craig-Chang [9], employ free interface modes, (residual) attachment modes, and rigid body modes and assemble the substructures in primal fashion as well. In contrast, the dual Craig-Bampton method [5] also employs free interface normal modes, (residual) attachment modes, and rigid body modes to build the substructures' reduction bases, but uses interface forces to assemble the substructures, which is referred to as dual assembly.

None of the aforementioned methods considers any damping effects when performing the reduction or, for simplification, proportional damping is assumed, which is the usual approach to damping [12]. If the damping properties are non-proportional (also called nonclassical) and damping significantly influences the dynamic behavior of the system under consideration, then the approximation accuracy of these methods can be very poor since the damping characteristics are represented inaccurately [13]. Hasselman [13] insisted that the assumption of a proportional damping model is inadequate to treat real systems [12]. There are many important instances in which these damping assumptions are not valid [14]. For example, structures with active control systems, with concentrated dampers or with rotational parts fall in this category [15]. Damping prediction, based on modal synthesis techniques utilizing only proportional damping information, is inappropriate [16]. This was demonstrated by Beliveau and Soucy [16] for the classical Craig-Bampton approach. Therefore, there is generally no justification to neglect damping properties for the computation of the reduction basis [13]. The fact that decoupling the damped equations of motion is not possible using classical modal analysis [17] will be highlighted in Section 2. One procedure to handle and decouple nonclassically damped systems is to transform the second-order differential equations into twice the number of first-order differential equations, resulting in state-space representation of the system, which was published by Frazer, Duncan and Collar [18] and made far clearer by Hurty and Rubinstein [19]. Solving the corresponding eigenvalue problem allows the damped equations of motion to be decoupled, but complex eigenmodes and eigenvalues will occur. Hasselman and Kaplan [20] presented a coupling procedure for damped systems, which is an extension of the Craig-Bampton method [1], which employs complex component modes. Beliveau and Soucy [16] proposed another version, which modifies the Craig-Bampton method to include damping by replacing the real fixed interface normal modes of the second-order system by the corresponding complex modes of the first-order system. Craig and Chung [14, 15] and Howsman and Craig [21] study various first-order formulations leading to complex component modes. Craig and Ni proposed a procedure for the application of complex free interface normal modes [22]. Brechlin and Gaul gave methodological improvements for the numerical implementation of dynamic substructuring methods [23]. A report of de Kraker [24] gives another description of the Craig-Bampton method for damped systems using complex normal modes. De Kraker and van Campen also generalized the Rubin method for general state-space models [25].

The dual Craig-Bampton method [5] is fundamentally different from the other methods in that it assem-

bles the substructures using interface forces (dual assembly) and enforces only weak interface compatibility. The reduced matrices associated to the dual Craig-Bampton method have a similar sparsity compared to the Craig-Bampton reduced matrices, but are less cumbersome (dense) than the reduced matrices obtained by other methods based on free interface modes [5]. Approximating eigenfrequencies, the dual Craig-Bampton method is outperforming the classical Craig-Bampton method using the same number of normal modes per substructure with comparable computational effort and having similar sparsity pattern for the reduced matrices [8]. The promising dual Craig-Bampton, which produces very good results for the approximation of undamped systems [5, 6, 8, 26, 27], has not yet been applied to damped systems. Therefore, we want to extend the dual Craig-Bampton method and demonstrate its potential for the case of nonclassically damped systems.

In this contribution, the original dual Craig-Bampton method for reducing and coupling undamped systems will be modified for general viscous damping. The final reduction is now based on the use of complex free interface normal modes, residual flexibility modes, and state-space rigid body modes. A dual coupling procedure based on the interface forces between adjacent substructures is used to couple substructures in state-space representation. This is novel compared to other methods, which commonly apply primal coupling procedures in state-space representation.

The traditional theory of decoupling by classical modal analysis is concisely surveyed in Section 2. The inadequacy of classical modal analysis for decoupling damped systems is also demonstrated. The terminology and notation used throughout this paper is set up. Section 3 recalls state-space representation and the corresponding decoupling procedure for damped systems. The original formulation of the dual Craig-Bampton method for undamped systems is shortly summarized in Section 4. In Section 5, the dual Craig-Bampton method for the undamped case is modified for the case of general viscous damping. A formulation in terms of first-order differential equations, i.e., state-space formulation, is presented for viscous damped systems. Floating substructures exhibiting rigid body modes will need special attention. The properties of the proposed method are subsequently illustrated in detail in Section 6 using a beam system with localized dampers as an illustrative application example. A comparison to the Craig-Bampton formulation for damped systems presented in [24] is made to demonstrate improvements of the proposed method. Finally, a brief summary of findings and conclusions is given in Section 7.

Appendix A summarizes the theory underlying the analysis of defective systems and of the Jordan normal. Since this theory is not common in the field of structural dynamics, we discuss it specifically with the objective to set the mathematical framework necessary for the analysis of state-space rigid body modes in damped systems in Appendix B.

2. Decoupling and inadequacy by classical modal analysis

Consider the equations of motion of a viscously damped linear system with m degrees of freedom (DOFs)

$$M\ddot{u} + C\dot{u} + Ku = f \tag{1}$$

with mass matrix M, damping matrix C, stiffness matrix K, displacement vector u, and external force vector f. Associated with the undamped system of Eq. (1), i.e., $C = 0$, is the eigenvalue problem

$$\left(-\omega_j^2 M + K\right) \theta_j = 0 \tag{2}$$

with eigenvalue ω_j^2 and corresponding eigenvector θ_j for $j = 1, \ldots, m$. The eigenvectors θ_j of Eq. (2) are called normal modes or natural modes and form the columns of the modal matrix Θ:

$$\Theta = \begin{bmatrix} \theta_1 & \theta_2 & \ldots & \theta_m \end{bmatrix} \tag{3}$$

If the modal matrix Θ is normalized with respect to the mass matrix M, then the normal modes' orthogonality conditions give

$$\Theta^{\mathrm{T}} M \Theta = I, \qquad \Theta^{\mathrm{T}} K \Theta = \Omega^2 = \mathrm{diag}\left(\omega_1^2, \, \omega_2^2, \, \ldots, \, \omega_m^2\right). \tag{4}$$

3

Using the modal transformation

$$\boldsymbol{u} = \boldsymbol{\Theta} \boldsymbol{p} \tag{5}$$

with the vector of modal coordinates $\boldsymbol{p}$, Eq. (1) takes the canonical form of the damped system [17]

$$\ddot{\boldsymbol{p}} + \boldsymbol{C}_{\text{modal}}\,\dot{\boldsymbol{p}} + \boldsymbol{\Omega}^2 \boldsymbol{p} = \boldsymbol{\Theta}^{\text{T}} \boldsymbol{f} \qquad \text{with} \qquad \boldsymbol{C}_{\text{modal}} = \boldsymbol{\Theta}^{\text{T}} \boldsymbol{C} \boldsymbol{\Theta}. \tag{6}$$

Mass matrix $\boldsymbol{M}$ and stiffness matrix $\boldsymbol{K}$ have been diagonalized by the modal transformation (5) and the diagonal eigenvalue matrix $\boldsymbol{\Omega}^2$ is given in Eq. (4). Matrix $\boldsymbol{C}_{\text{modal}}$ is referred to as generalized damping matrix or modal damping matrix [6]. Any modal coupling in a linear system occurs exclusively through damping [28]. A damped system is called classically damped if it can be decoupled by the modal matrix $\boldsymbol{\Theta}$ [6], i.e., $\boldsymbol{C}_{\text{modal}}$ is also diagonalized by the modal transformation (5). A necessary and sufficient condition that the damped system can be decoupled and hence that the damping matrix $\boldsymbol{C}$ can be diagonalized by the modal matrix $\boldsymbol{\Theta}$ is [29]:

$$\boldsymbol{C} \boldsymbol{M}^{-1} \boldsymbol{K} = \boldsymbol{K} \boldsymbol{M}^{-1} \boldsymbol{C} \tag{7}$$

Condition (7) is usually not satisfied. Only under special conditions are the equations of motion completely diagonalized by the classical modal transformation [17], and these conditions appear to have little physical justification [13]. For instance, the often used but simplifying assumptions of mass proportional damping, stiffness proportional damping, Rayleigh damping [30], or modal damping fulfill condition (7) and diagonalize the generalized damping matrix $\boldsymbol{C}_{\text{modal}}$. Nevertheless, decoupling of Eq. (1) is not generally possible using classical modal analysis.

3. State-space representation and decoupling of damped systems

A procedure to handle and decouple systems that are not classically damped, i.e., systems with general viscous damping, is to transform the m second-order equations of motion (1) into $2m$ first-order equations [6, 18, 19, 31]. The state-space vector of dimension $n = 2m$ is

$$\boldsymbol{z}(t) = \begin{bmatrix} \boldsymbol{u}(t) \\ \boldsymbol{v}(t) \end{bmatrix} \tag{8}$$

with $\boldsymbol{v}(t) = \dot{\boldsymbol{u}}(t)$. Adding the m redundant equations $\boldsymbol{M} \boldsymbol{v}(t) = \boldsymbol{M} \dot{\boldsymbol{u}}(t)$ to the equations of motion (1), the generalized state-space symmetric form

$$\mathcal{A} \dot{\boldsymbol{z}} + \mathcal{B} \boldsymbol{z} = \mathcal{F} \tag{9}$$

is obtained with

$$\mathcal{A} = \begin{bmatrix} \boldsymbol{C} & \boldsymbol{M} \\ \boldsymbol{M} & \boldsymbol{0} \end{bmatrix}, \qquad \mathcal{B} = \begin{bmatrix} \boldsymbol{K} & \boldsymbol{0} \\ \boldsymbol{0} & -\boldsymbol{M} \end{bmatrix}, \qquad \mathcal{F} = \begin{bmatrix} \boldsymbol{f} \\ \boldsymbol{0} \end{bmatrix}. \tag{10}$$

Associated with Eq. (9), which includes the damping matrix $\boldsymbol{C}$, is the eigenvalue problem

$$(\sigma_j \mathcal{A} + \mathcal{B})\,\boldsymbol{\theta}_{\text{ss},j} = \boldsymbol{0} \tag{11}$$

with eigenvalue σ_j and corresponding state-space eigenvector $\boldsymbol{\theta}_{\text{ss},j}$ for $j = 1, \ldots, n$. Since matrices $\mathcal{A}$ and $\mathcal{B}$ are real, the n eigenvalues σ_j must either be real or they must occur in complex conjugate pairs [19]. For underdamped systems, the eigenvalues σ_j and corresponding eigenmodes $\boldsymbol{\theta}_{\text{ss},j}$ occur in complex conjugate pairs [12] and are called underdamped eigenvalues and underdamped eigenmodes, respectively[1]. Since real eigenvalues indicate very high damping leading to overdamped modes, most structures have m complex conjugate pairs of eigenvalues and corresponding eigenvectors [6]. The eigenvectors $\boldsymbol{\theta}_{\text{ss},j}$ are therefore referred to as complex normal modes.

---

[1] Overdamped and underdamped mode refer, respectively, to a mode with damping above and below the critical damping [19].

Similar to the undamped case in Eq. (3), the state-space eigenvectors $\boldsymbol{\theta}_{\mathrm{ss},j}$ form the complex state-space modal matrix

$$\boldsymbol{\Theta}_{\mathrm{ss}} = \begin{bmatrix} \boldsymbol{\theta}_{\mathrm{ss},1} & \boldsymbol{\theta}_{\mathrm{ss},2} & \ldots & \boldsymbol{\theta}_{\mathrm{ss},n} \end{bmatrix}. \tag{12}$$

An extensive investigation of properties and relations between complex normal modes of Eq. (12) and real normal modes of Eq. (3) is given in [32]. If the complex modal matrix $\boldsymbol{\Theta}_{\mathrm{ss}}$ is normalized with respect to the state-space matrix $\boldsymbol{\mathcal{A}}$, the orthogonality conditions of the complex normal modes give

$$\boldsymbol{\Theta}_{\mathrm{ss}}^{\mathrm{T}} \boldsymbol{\mathcal{A}} \boldsymbol{\Theta}_{\mathrm{ss}} = \boldsymbol{I}, \qquad \boldsymbol{\Theta}_{\mathrm{ss}}^{\mathrm{T}} \boldsymbol{\mathcal{B}} \boldsymbol{\Theta}_{\mathrm{ss}} = -\boldsymbol{\Sigma} = -\mathrm{diag}\left(\sigma_1, \, \sigma_2, \, \ldots, \, \sigma_n\right). \tag{13}$$

Complex modal matrix $\boldsymbol{\Theta}_{\mathrm{ss}}$ decouples the damped system if it is written in state-space format as in Eq. (9). For the orthogonality conditions in Eq. (13), it is assumed that the system Eq. (9) is non-defective. The special case of defective systems is illustrated in detail in Appendix A and has to be considered in Section 5 to include state-space rigid body motion.

4. Dual Craig-Bampton method

In this section, we briefly summarize the dual Craig-Bampton method for undamped structures [5], which will subsequently be extended in Section 5 for the damped case. Consider a domain that is divided into N non-overlapping substructures such that every node belongs to exactly one substructure except for the nodes on the interface boundaries. The undamped equations of motion of one substructure s are

$$\boldsymbol{M}^{(s)} \ddot{\boldsymbol{u}}^{(s)} + \boldsymbol{K}^{(s)} \boldsymbol{u}^{(s)} = \boldsymbol{f}^{(s)} + \boldsymbol{g}^{(s)}, \qquad s = 1, \ldots, N. \tag{14}$$

Eq. (14) has $m^{(s)}$ DOFs and the superscript (s) is the label of the particular substructure s. $\boldsymbol{g}^{(s)}$ is the vector of internal forces connecting adjacent substructures at their boundary DOFs.

4.1. Dual assembly

One way to enforce interface compatibility between the different substructures is to consider the interface connecting forces $\boldsymbol{g}^{(s)}$ as unknowns. These forces must be determined to satisfy the interface compatibility condition (displacement equality) and the local equations of motion of the substructures:

$$\sum_{s=1}^{N} \boldsymbol{B}^{(s)} \boldsymbol{u}^{(s)} = \boldsymbol{0} \tag{15}$$

$$\boldsymbol{M}^{(s)} \ddot{\boldsymbol{u}}^{(s)} + \boldsymbol{K}^{(s)} \boldsymbol{u}^{(s)} + \boldsymbol{B}^{(s)^{\mathrm{T}}} \boldsymbol{\lambda} = \boldsymbol{f}^{(s)}, \qquad s = 1, \ldots, N \tag{16}$$

$\boldsymbol{B}^{(s)}$ is a signed Boolean matrix expressing the interface compatibility for the substructure DOFs $\boldsymbol{u}^{(s)}$. Vector $\boldsymbol{B}^{(s)^{\mathrm{T}}} \boldsymbol{\lambda}$ represents the interconnecting forces between substructures, which corresponds to the negative interface reaction force vector $\boldsymbol{g}^{(s)}$ in Eq. (14). This means

$$\boldsymbol{g}^{(s)} = -\boldsymbol{B}^{(s)^{\mathrm{T}}} \boldsymbol{\lambda}, \tag{17}$$

where $\boldsymbol{\lambda}$ is the vector of all Lagrange multipliers acting on the interfaces, which are the additional unknowns. Using the block-diagonal matrices

$$\boldsymbol{M}_{\mathrm{bd}} = \begin{bmatrix} \boldsymbol{M}^{(1)} & & \boldsymbol{0} \\ & \ddots & \\ \boldsymbol{0} & & \boldsymbol{M}^{(N)} \end{bmatrix}, \quad \boldsymbol{K}_{\mathrm{bd}} = \begin{bmatrix} \boldsymbol{K}^{(1)} & & \boldsymbol{0} \\ & \ddots & \\ \boldsymbol{0} & & \boldsymbol{K}^{(N)} \end{bmatrix}, \tag{18}$$

the corresponding partitioned, concatenated vectors

$$\boldsymbol{u}_{\mathrm{bd}} = \begin{bmatrix} \boldsymbol{u}^{(1)} \\ \vdots \\ \boldsymbol{u}^{(N)} \end{bmatrix}, \quad \boldsymbol{f}_{\mathrm{bd}} = \begin{bmatrix} \boldsymbol{f}^{(1)} \\ \vdots \\ \boldsymbol{f}^{(N)} \end{bmatrix} \tag{19}$$

and Boolean matrix

$$\boldsymbol{B} = \begin{bmatrix} \boldsymbol{B}^{(1)} & \cdots & \boldsymbol{B}^{(N)} \end{bmatrix}, \tag{20}$$

substructure Eqs. (15) and (16) can be assembled as

$$\begin{bmatrix} \boldsymbol{M}_{\mathrm{bd}} & \boldsymbol{0} \\ \boldsymbol{0} & \boldsymbol{0} \end{bmatrix} \begin{bmatrix} \ddot{\boldsymbol{u}}_{\mathrm{bd}} \\ \ddot{\boldsymbol{\lambda}} \end{bmatrix} + \begin{bmatrix} \boldsymbol{K}_{\mathrm{bd}} & \boldsymbol{B}^{\mathrm{T}} \\ \boldsymbol{B} & \boldsymbol{0} \end{bmatrix} \begin{bmatrix} \boldsymbol{u}_{\mathrm{bd}} \\ \boldsymbol{\lambda} \end{bmatrix} = \begin{bmatrix} \boldsymbol{f}_{\mathrm{bd}} \\ \boldsymbol{0} \end{bmatrix}. \tag{21}$$

$\boldsymbol{B}$ is referred to as the constraint matrix [6] and Eq. (21) is referred to as dual assembled system. In this hybrid formulation, the Lagrange multipliers $\boldsymbol{\lambda}$ enforce the interface compatibility constraints and can be identified as interface forces [5]. Constraint matrix $\boldsymbol{B}$ is a signed Boolean matrix if the interface degrees of freedom are matching, i.e., for matching (conforming) mesh-conditions on the interfaces between the substructures [33]. If adjacent substructures do not have matching mesh-conditions on the interfaces (e.g., if substructures do not originate from a partitioning of a global mesh and are meshed independently), the interface compatibility is usually enforced through nodal collocation or by using weak interface compatibility formulations [33, 34, 35]. Then, the compatibility condition can still be written as $\boldsymbol{B}\boldsymbol{u}_{\mathrm{bd}} = \boldsymbol{0}$ but $\boldsymbol{B}$ is no longer Boolean [6, 33, 36].

4.2. Reduction of dual assembled system

Considering the equations of motion (16) of substructure s without external forces $\boldsymbol{f}^{(s)}$, every substructure can be seen as being excited by the interface connection forces $\boldsymbol{\lambda}$. This indicates that the local dynamic behavior can be described by superposing local static and local dynamic modes. The displacements $\boldsymbol{u}^{(s)}$ of each substructure are expressed in terms of local static solutions $\boldsymbol{u}_{\mathrm{stat}}^{(s)}$ and in terms of eigenmodes associated with the substructure matrices $\boldsymbol{K}^{(s)}$ and $\boldsymbol{M}^{(s)}$:

$$\boldsymbol{u}^{(s)} = \boldsymbol{u}_{\mathrm{stat}}^{(s)} + \sum_{j=1}^{m^{(s)}-m_r^{(s)}} \boldsymbol{\theta}_j^{(s)} p_j^{(s)} \qquad \text{with} \qquad \boldsymbol{u}_{\mathrm{stat}}^{(s)} = -\boldsymbol{K}^{(s)^+} \boldsymbol{B}^{(s)\mathrm{T}} \boldsymbol{\lambda} + \sum_{j=1}^{m_r^{(s)}} \boldsymbol{r}_j^{(s)} \alpha_j^{(s)}. \tag{22}$$

$m^{(s)}$ is the dimension of the local substructure problem. Matrix $\boldsymbol{K}^{(s)^+}$ is equal to the inverse of $\boldsymbol{K}^{(s)}$ if there are enough boundary conditions to prevent the substructure from floating when its interface with adjacent substructures is free [5]. If a substructure is floating, then the generalized inverse $\boldsymbol{K}^{(s)^+}$ has to be used and

$$\boldsymbol{R}^{(s)} = \begin{bmatrix} \boldsymbol{r}_1^{(s)} & \boldsymbol{r}_2^{(s)} & \dots & \boldsymbol{r}_{m_r}^{(s)} \end{bmatrix} \tag{23}$$

is the matrix containing the $m_r^{(s)}$ rigid body modes $\boldsymbol{r}_j^{(s)}$ as columns, which are assumed to be orthonormalized with respect to the mass matrix $\boldsymbol{M}^{(s)}$. Vector $\boldsymbol{\alpha}^{(s)}$ contains the amplitudes $\alpha_j^{(s)}$ of the rigid body modes $\boldsymbol{r}_j^{(s)}$. The flexibility matrix $\boldsymbol{G}^{(s)}$ in inertia-relief format is computed from any generalized inverse $\boldsymbol{K}^{(s)^+}$ by projecting out the rigid body modes $\boldsymbol{R}^{(s)}$ using the inertia-relief projection matrix $\boldsymbol{P}^{(s)}$ which is defined as [6, 37]

$$\boldsymbol{P}^{(s)} = \boldsymbol{I}^{(s)} - \boldsymbol{M}^{(s)} \boldsymbol{R}^{(s)} \boldsymbol{R}^{(s)\mathrm{T}} \tag{24}$$

and therefore

$$\boldsymbol{G}^{(s)} = \boldsymbol{P}^{(s)\mathrm{T}} \boldsymbol{K}^{(s)^+} \boldsymbol{P}^{(s)}. \tag{25}$$

The amplitudes $p_j^{(s)}$ of the local eigenmodes $\boldsymbol{\theta}_j^{(s)}$ in Eq. (22) are grouped in the vector $\boldsymbol{p}^{(s)}$. The local eigenmodes $\boldsymbol{\theta}_j^{(s)}$ satisfy the generalized eigenproblem

$$\left(-\omega_j^{(s)^2} \boldsymbol{M}^{(s)} + \boldsymbol{K}^{(s)} \right) \boldsymbol{\theta}_j^{(s)} = \boldsymbol{0}. \tag{26}$$

The eigenmodes $\boldsymbol{\theta}_j^{(s)}$ are also called free interface normal modes and are orthonormalized with respect to the mass matrix $\boldsymbol{M}^{(s)}$. An approximation of the general solution (22) is obtained by retaining only the first $m_\theta^{(s)}$ free interface normal modes $\boldsymbol{\theta}_j^{(s)}$ corresponding to the $m_\theta^{(s)}$ lowest eigenvalues $\omega_j^{(s)^2}$. Calling $\tilde{\boldsymbol{\Theta}}^{(s)}$ the matrix containing these eigenmodes, the approximation of the displacements $\boldsymbol{u}^{(s)}$ of the substructure is written as

$$\boldsymbol{u}^{(s)} \approx -\boldsymbol{G}^{(s)}\boldsymbol{B}^{(s)^\mathrm{T}}\boldsymbol{\lambda} + \boldsymbol{R}^{(s)}\boldsymbol{\alpha}^{(s)} + \tilde{\boldsymbol{\Theta}}^{(s)}\boldsymbol{p}^{(s)}. \tag{27}$$

Matrix $\tilde{\boldsymbol{\Theta}}^{(s)}$ of kept eigenmodes satisfies

$$\tilde{\boldsymbol{\Theta}}^{(s)^\mathrm{T}}\boldsymbol{M}^{(s)}\tilde{\boldsymbol{\Theta}}^{(s)} = \boldsymbol{I} \quad\text{and}\quad \tilde{\boldsymbol{\Theta}}^{(s)^\mathrm{T}}\boldsymbol{K}^{(s)}\tilde{\boldsymbol{\Theta}}^{(s)} = \boldsymbol{\Omega}^{(s)^2} = \mathrm{diag}\left(\omega_1^{(s)^2}, \omega_2^{(s)^2}, \ldots, \omega_{m_\theta}^{(s)^2}\right) \tag{28}$$

with $\boldsymbol{\Omega}^{(s)}$ being a diagonal matrix containing the $m_\theta^{(s)}$ eigenvalues $\omega_j^{(s)}$ corresponding to the kept free interface normal modes $\boldsymbol{\theta}_j^{(s)}$. Since a part of the subspace spanned by $\tilde{\boldsymbol{\Theta}}^{(s)}$ is already included in $\boldsymbol{G}^{(s)}$, residual flexibility matrix $\boldsymbol{G}_\mathrm{res}^{(s)}$ can be used instead of flexibility matrix $\boldsymbol{G}^{(s)}$. The residual flexibility matrix $\boldsymbol{G}_\mathrm{res}^{(s)}$ is defined by

$$\boldsymbol{G}_\mathrm{res}^{(s)} = \sum_{j=m_\theta^{(s)}+1}^{m^{(s)}-m_r^{(s)}} \frac{\boldsymbol{\theta}_j^{(s)}\boldsymbol{\theta}_j^{(s)^\mathrm{T}}}{\omega_j^{(s)^2}} = \boldsymbol{G}^{(s)} - \sum_{j=1}^{m_\theta^{(s)}} \frac{\boldsymbol{\theta}_j^{(s)}\boldsymbol{\theta}_j^{(s)^\mathrm{T}}}{\omega_j^{(s)^2}}. \tag{29}$$

Note that by construction $\boldsymbol{G}_\mathrm{res}^{(s)} = \boldsymbol{G}_\mathrm{res}^{(s)^\mathrm{T}}$, which is computed using the second equality in Eq. (29). For further properties of $\boldsymbol{G}_\mathrm{res}^{(s)}$ see [5, 26]. As a result, the approximation of one substructure is

$$\boldsymbol{u}^{(s)} \approx -\boldsymbol{G}_\mathrm{res}^{(s)}\boldsymbol{B}^{(s)^\mathrm{T}}\boldsymbol{\lambda} + \boldsymbol{R}^{(s)}\boldsymbol{\alpha}^{(s)} + \tilde{\boldsymbol{\Theta}}^{(s)}\boldsymbol{p}^{(s)} = \begin{bmatrix} \boldsymbol{R}^{(s)} & \tilde{\boldsymbol{\Theta}}^{(s)} & -\boldsymbol{G}_\mathrm{res}^{(s)}\boldsymbol{B}^{(s)^\mathrm{T}} \end{bmatrix} \begin{bmatrix} \boldsymbol{\alpha}^{(s)} \\ \boldsymbol{p}^{(s)} \\ \boldsymbol{\lambda} \end{bmatrix}. \tag{30}$$

Assembling all N substructures in a dual fashion according to Eq. (21) by keeping the interface forces $\boldsymbol{\lambda}$ as unknowns, the DOFs of the entire structure can consequently be approximated by

$$\begin{bmatrix} \boldsymbol{u}_\mathrm{bd} \\ \boldsymbol{\lambda} \end{bmatrix} \approx \underbrace{\begin{bmatrix} \boldsymbol{R}^{(1)} & \tilde{\boldsymbol{\Theta}}^{(1)} & & \boldsymbol{0} & \boldsymbol{0} & -\boldsymbol{G}_\mathrm{res}^{(1)}\boldsymbol{B}^{(1)^\mathrm{T}} \\ & & \ddots & \ddots & & \vdots \\ \boldsymbol{0} & \boldsymbol{0} & & \boldsymbol{R}^{(N)} & \tilde{\boldsymbol{\Theta}}^{(N)} & -\boldsymbol{G}_\mathrm{res}^{(N)}\boldsymbol{B}^{(N)^\mathrm{T}} \\ \boldsymbol{0} & \boldsymbol{0} & & \boldsymbol{0} & \boldsymbol{0} & \boldsymbol{I} \end{bmatrix}}_{\boldsymbol{T}_\mathrm{DCB}} \begin{bmatrix} \boldsymbol{\alpha}^{(1)} \\ \boldsymbol{p}^{(1)} \\ \vdots \\ \boldsymbol{\alpha}^{(N)} \\ \boldsymbol{p}^{(N)} \\ \boldsymbol{\lambda} \end{bmatrix}. \tag{31}$$

Matrix $\boldsymbol{T}_\mathrm{DCB}$ is the dual Craig-Bampton reduction matrix. The approximation of the dual assembled system's dynamic equations (21) is

$$\boldsymbol{M}_\mathrm{DCB} \begin{bmatrix} \ddot{\boldsymbol{\alpha}}^{(1)} \\ \ddot{\boldsymbol{p}}^{(1)} \\ \vdots \\ \ddot{\boldsymbol{\alpha}}^{(N)} \\ \ddot{\boldsymbol{p}}^{(N)} \\ \ddot{\boldsymbol{\lambda}} \end{bmatrix} + \boldsymbol{K}_\mathrm{DCB} \begin{bmatrix} \boldsymbol{\alpha}^{(1)} \\ \boldsymbol{p}^{(1)} \\ \vdots \\ \boldsymbol{\alpha}^{(N)} \\ \boldsymbol{p}^{(N)} \\ \boldsymbol{\lambda} \end{bmatrix} = \boldsymbol{f}_\mathrm{DCB} \tag{32}$$

with

$$\boldsymbol{M}_\mathrm{DCB} = \boldsymbol{T}_\mathrm{DCB}^\mathrm{T} \begin{bmatrix} \boldsymbol{M}_\mathrm{bd} & \boldsymbol{0} \\ \boldsymbol{0} & \boldsymbol{0} \end{bmatrix} \boldsymbol{T}_\mathrm{DCB}, \quad \boldsymbol{K}_\mathrm{DCB} = \boldsymbol{T}_\mathrm{DCB}^\mathrm{T} \begin{bmatrix} \boldsymbol{K}_\mathrm{bd} & \boldsymbol{B}^\mathrm{T} \\ \boldsymbol{B} & \boldsymbol{0} \end{bmatrix} \boldsymbol{T}_\mathrm{DCB}, \quad \boldsymbol{f}_\mathrm{DCB} = \boldsymbol{T}_\mathrm{DCB}^\mathrm{T} \begin{bmatrix} \boldsymbol{f}_\mathrm{bd} \\ \boldsymbol{0} \end{bmatrix}. \tag{33}$$

The dual Craig-Bampton reduced system has the final size of $m_{\mathrm{DCB}} = \sum_{s=1}^{N} m_r^{(s)} + \sum_{s=1}^{N} m_\theta^{(s)} + m_\lambda$ DOFs with $m_r^{(s)}$ rigid body modes of substructure s, with $m_\theta^{(s)}$ kept free interface normal modes of substructure s, and with the total number m_λ of all Lagrange multipliers [5, 8].

The dual Craig-Bampton method [5] for undamped systems is fundamentally different from the other methods in that it assembles the substructures using interface forces and enforces only weak interface compatibility. Approximating eigenfrequencies, the dual Craig-Bampton method is outperforming most of the other methods using the same number of normal modes per substructure with comparable computational effort and having similar sparsity pattern for the reduced matrices [5, 8, 26, 27]. Non-physical spurious negative eigenvalues and corresponding eigenvectors of the reduced dual assembled problem are intrinsic in the reduction process using the dual Craig-Bampton method caused by the weak compatibility on the interfaces between the substructures [5, 26, 42]. The weakening of the compatibility was shown to avoid interface locking problems, but has the consequence to introduce contributions of the Lagrange multipliers to the reduced mass matrix. This does not influence the very good approximation accuracy of the eigenvalues and eigenvectors [5, 6, 27], but it can cause problems in some applications (e.g., time integration). For the original formulation of the dual Craig-Bampton method [5], a time integration strategy is investigated in [43].

5. Dual Craig-Bampton method for general state-space models

Consider again a domain, which is divided into N non-overlapping substructures, as in Section 4. The equations of motion of one viscously damped linear substructure s with $m^{(s)}$ DOFs are

$$\boldsymbol{M}^{(s)}\ddot{\boldsymbol{u}}^{(s)} + \boldsymbol{C}^{(s)}\dot{\boldsymbol{u}}^{(s)} + \boldsymbol{K}^{(s)}\boldsymbol{u}^{(s)} = \boldsymbol{f}^{(s)} + \boldsymbol{g}^{(s)}, \qquad s = 1, \ldots, N, \tag{34}$$

which will be considered in the following instead of the undamped equations of motion (14). $\boldsymbol{C}^{(s)}$ is the substructure's damping matrix. The substructure state-space vector $\boldsymbol{z}^{(s)}$ of dimension $n^{(s)} = 2m^{(s)}$ is

$$\boldsymbol{z}^{(s)} = \begin{bmatrix} \boldsymbol{u}^{(s)} \\ \boldsymbol{v}^{(s)} \end{bmatrix} \tag{35}$$

with $\boldsymbol{v}^{(s)} = \dot{\boldsymbol{u}}^{(s)}$. The corresponding generalized equations of motion in state-space form are

$$\boldsymbol{\mathcal{A}}^{(s)}\dot{\boldsymbol{z}}^{(s)} + \boldsymbol{\mathcal{B}}^{(s)}\boldsymbol{z}^{(s)} = \boldsymbol{\mathcal{F}}^{(s)} \tag{36}$$

with

$$\boldsymbol{\mathcal{A}}^{(s)} = \begin{bmatrix} \boldsymbol{C}^{(s)} & \boldsymbol{M}^{(s)} \\ \boldsymbol{M}^{(s)} & \boldsymbol{0} \end{bmatrix}, \qquad \boldsymbol{\mathcal{B}}^{(s)} = \begin{bmatrix} \boldsymbol{K}^{(s)} & \boldsymbol{0} \\ \boldsymbol{0} & -\boldsymbol{M}^{(s)} \end{bmatrix}, \qquad \boldsymbol{\mathcal{F}}^{(s)} = \begin{bmatrix} \boldsymbol{f}^{(s)} + \boldsymbol{g}^{(s)} \\ \boldsymbol{0} \end{bmatrix}. \tag{37}$$

As outlined in Section 4, the dual Craig-Bampton method is based on free interface normal modes, rigid body modes, and residual flexibility modes. Each substructure's local behavior is approximated by superposing static and dynamic parts. Now we want to approximate the state-space vector $\boldsymbol{z}^{(s)}$ of substructure s by a superposition of a static response $\boldsymbol{z}_{\mathrm{stat}}^{(s)}$ and a dynamic part $\boldsymbol{z}_{\mathrm{dyn}}^{(s)}$ similar to Eq. (22):

$$\boldsymbol{z}^{(s)} = \boldsymbol{z}_{\mathrm{stat}}^{(s)} + \boldsymbol{z}_{\mathrm{dyn}}^{(s)} \tag{38}$$

Static response $\boldsymbol{z}_{\mathrm{stat}}^{(s)}$ is associated with the interface excitation and dynamic part $\boldsymbol{z}_{\mathrm{dyn}}^{(s)}$ is associated with the substructure matrices' eigenmodes.

If a substructure is floating, the stiffness matrix $\boldsymbol{K}^{(s)}$ is singular and the second-order system with corresponding equations of motion (14) has $m_r^{(s)}$ physical rigid body DOFs. The corresponding physical rigid body modes $\boldsymbol{R}^{(s)}$ fulfill the condition

$$\boldsymbol{K}^{(s)}\boldsymbol{R}^{(s)} = \boldsymbol{0}. \tag{39}$$

8

The eigenvalue problem of the state-space equations of motion (36) is

$$\left(\sigma_j^{(s)} \boldsymbol{\mathcal{A}}^{(s)} + \boldsymbol{\mathcal{B}}^{(s)}\right) \boldsymbol{\theta}_{\text{ss},j}^{(s)} = \mathbf{0}. \tag{40}$$

It can be shown that the existence of $m_r^{(s)}$ physical rigid body modes according to Eq. (39) leads to $n_r^{(s)}$ eigenvalues $\sigma_j^{(s)}$ of the eigenvalue problem in Eq. (40) equal to zero [38] and $m_r^{(s)} \leq n_r^{(s)} \leq 2m_r^{(s)}$ holds for the $n_r^{(s)}$ zero eigenvalues of the state-space eigenproblem [25]. For details see Appendix A and Appendix B. Using the physical rigid body modes $\boldsymbol{r}_j^{(s)}$, it is shown in Appendix B that two situations can exist for each physical rigid body mode $\boldsymbol{r}_j^{(s)}$ [25, 39]:

- Situation 1: $\boldsymbol{C}^{(s)} \boldsymbol{r}_j^{(s)} = \mathbf{0}$

  In this case an eigenvalue $\sigma_j^{(s)} = 0$ with multiplicity two leads to one regular eigenvector $\boldsymbol{r}_{\text{ss},j,\text{reg}}^{(s)}$ and one generalized eigenvector $\boldsymbol{r}_{\text{ss},j,\text{gen}}^{(s)}$. This regular eigenvector $\boldsymbol{r}_{\text{ss},j,\text{reg}}^{(s)}$ and the generalized eigenvector $\boldsymbol{r}_{\text{ss},j,\text{gen}}^{(s)}$ both correspond to the physical rigid body mode $\boldsymbol{r}_j^{(s)}$. This is the case for undamped systems, but it can also be valid for damped systems [25] if the condition $\boldsymbol{C}^{(s)} \boldsymbol{r}_j^{(s)} = \mathbf{0}$ is fulfilled. In the situation considered here, matrix $\boldsymbol{\Sigma}^{(s)}$ will not be diagonal but has a Jordan normal form having Jordan blocks on the diagonal [23, 38]. The system is called defective. For details see Appendix A.

- Situation 2: $\boldsymbol{C}^{(s)} \boldsymbol{r}_j^{(s)} \neq \mathbf{0}$

  The system is non-defective for the physical rigid body mode $\boldsymbol{r}_j^{(s)}$ and there is only one regular eigenvector $\boldsymbol{r}_{\text{ss},j,\text{reg}}^{(s)}$ and no generalized eigenvector $\boldsymbol{r}_{\text{ss},j,\text{gen}}^{(s)}$ corresponding to $\sigma_j^{(s)} = 0$. This eigenvalue $\sigma_j^{(s)} = 0$ is a single non-repeated root. Only one regular eigenvector $\boldsymbol{r}_{\text{ss},j,\text{reg}}^{(s)}$ corresponds to the physical rigid body mode $\boldsymbol{r}_j^{(s)}$. In this situation, the corresponding part of matrix $\boldsymbol{\Sigma}^{(s)}$ will be a scalar term that is the single eigenvalue $\sigma_j^{(s)} = 0$. $\boldsymbol{\Sigma}^{(s)}$ will thus be diagonal.

5.1. Dynamic part of the solution

The solution of the eigenproblem (40) gives $n^{(s)} = 2m^{(s)}$ eigenvalues $\sigma_j^{(s)}$, $j = 1, \ldots, n^{(s)}$ including zero eigenvalues and $n^{(s)}$ corresponding eigenvectors $\boldsymbol{\theta}_{\text{ss},j}^{(s)}$. By analogy with the substructure state-space vector in Eq. (35), state-space eigenvectors $\boldsymbol{\theta}_{\text{ss},j}^{(s)}$ have the form

$$\boldsymbol{\theta}_{\text{ss},j}^{(s)} = \begin{bmatrix} \boldsymbol{\theta}_{\text{ss},j,u}^{(s)} \\ \boldsymbol{\theta}_{\text{ss},j,v}^{(s)} \end{bmatrix} = \begin{bmatrix} \boldsymbol{\theta}_{\text{ss},j,u}^{(s)} \\ \sigma_j^{(s)} \boldsymbol{\theta}_{\text{ss},j,u}^{(s)} \end{bmatrix}. \tag{41}$$

Some of these eigenvectors can be used to span a subspace to approximate the substructure's state-space vector $\boldsymbol{z}^{(s)}$. If the substructure has rigid body DOFs and generalized state-space rigid body modes $\boldsymbol{R}_{\text{ss},\text{gen}}^{(s)}$ occur, the Jordan form has to be used since the eigenmodes of Eq. (40) corresponding to eigenvalues $\sigma_j^{(s)} = 0$ will not diagonalize the system. If only regular state-space rigid body modes $\boldsymbol{R}_{\text{ss},\text{reg}}^{(s)}$ show up, the substructure matrices $\boldsymbol{\mathcal{A}}^{(s)}$ and $\boldsymbol{\mathcal{B}}^{(s)}$ can be transformed to diagonal form. The $n^{(s)} - n_r^{(s)}$ state-space eigenmodes $\boldsymbol{\theta}_{\text{ss},j}^{(s)}$ corresponding to eigenvalues $\sigma_j^{(s)} \neq 0$ are written as columns of the matrix $\boldsymbol{\Theta}_{\text{ss}}^{(s)}$. The modes contained in $\boldsymbol{\Theta}_{\text{ss}}^{(s)}$ are orthonormalized with respect to matrix $\boldsymbol{\mathcal{A}}^{(s)}$, so that they satisfy the following orthogonality equations for complex modes:

$$\boldsymbol{\Theta}_{\text{ss}}^{(s)^{\text{T}}} \boldsymbol{\mathcal{A}}^{(s)} \boldsymbol{\Theta}_{\text{ss}}^{(s)} = \boldsymbol{I}, \qquad \boldsymbol{\Theta}_{\text{ss}}^{(s)^{\text{T}}} \boldsymbol{\mathcal{B}}^{(s)} \boldsymbol{\Theta}_{\text{ss}}^{(s)} = -\boldsymbol{\Sigma}^{(s)} = -\text{diag}\left(\sigma_1^{(s)}, \sigma_2^{(s)}, \ldots, \sigma_{n-n_r}^{(s)}\right) \tag{42}$$

The first $n_\theta^{(s)}$ normal modes $\boldsymbol{\theta}_{\text{ss},j}^{(s)}$ corresponding to the $n_\theta^{(s)}$ lowest nonzero eigenvalues $\sigma_j^{(s)}$ are retained as part of the reduction basis of the substructure to approximate the dynamic part $\boldsymbol{z}_{\text{dyn}}^{(s)}$ of the state-space

9

vector $\boldsymbol{z}^{(s)}$ in Eq. (38). Matrix $\tilde{\boldsymbol{\Theta}}_{\mathrm{ss}}^{(s)}$ contains those first $n_\theta^{(s)}$ normal modes $\boldsymbol{\theta}_{\mathrm{ss},j}^{(s)}$ as columns. Thus the approximation of the dynamic part $\boldsymbol{z}_{\mathrm{dyn}}^{(s)}$ is

$$\boldsymbol{z}_{\mathrm{dyn}}^{(s)} \approx \sum_{j=1}^{n_\theta^{(s)}} \boldsymbol{\theta}_{\mathrm{ss},j}^{(s)} p_j^{(s)} = \begin{bmatrix} \boldsymbol{\theta}_{\mathrm{ss},1}^{(s)} & \boldsymbol{\theta}_{\mathrm{ss},2}^{(s)} & \cdots & \boldsymbol{\theta}_{\mathrm{ss},n_\theta}^{(s)} \end{bmatrix} \boldsymbol{p}^{(s)} = \tilde{\boldsymbol{\Theta}}_{\mathrm{ss}}^{(s)} \boldsymbol{p}^{(s)}. \tag{43}$$

5.2. Static part of the solution

The substructure's static solution $\boldsymbol{z}_{\mathrm{stat}}^{(s)}$ is obtained in a way similar to that of the undamped case: rigid body modes and residual attachment modes are superposed. To this end, the static substructure equation

$$\boldsymbol{\mathcal{B}}^{(s)} \boldsymbol{z}_{\mathrm{stat}}^{(s)} = \boldsymbol{\mathcal{F}}^{(s)} = \begin{bmatrix} \boldsymbol{g}^{(s)} \\ \boldsymbol{0} \end{bmatrix} \tag{44}$$

is considered, which follows from Eq. (36) by setting $\dot{\boldsymbol{z}}^{(s)} = \boldsymbol{0}$ for the time derivative of state-space vector $\boldsymbol{z}^{(s)}$ and assuming only forces $\boldsymbol{g}^{(s)}$ due to adjacent substructures. If the substructure has no rigid body DOFs, then the inverse of $\boldsymbol{\mathcal{B}}^{(s)}$ exists and the static solution is

$$\boldsymbol{z}_{\mathrm{stat}}^{(s)} = \boldsymbol{\mathcal{B}}^{(s)^{-1}} \boldsymbol{\mathcal{F}}^{(s)} = \begin{bmatrix} \boldsymbol{K}^{(s)^{-1}} & \boldsymbol{0} \\ \boldsymbol{0} & -\boldsymbol{M}^{(s)^{-1}} \end{bmatrix} \begin{bmatrix} \boldsymbol{g}^{(s)} \\ \boldsymbol{0} \end{bmatrix} = -\begin{bmatrix} \boldsymbol{K}^{(s)^{-1}} & \boldsymbol{0} \\ \boldsymbol{0} & -\boldsymbol{M}^{(s)^{-1}} \end{bmatrix} \begin{bmatrix} \boldsymbol{B}^{(s)^{\mathrm{T}}} \boldsymbol{\lambda} \\ \boldsymbol{0} \end{bmatrix}. \tag{45}$$

In Eq. (45), the vector of interface forces $\boldsymbol{g}^{(s)}$ is replaced by the relation $\boldsymbol{g}^{(s)} = -\boldsymbol{B}^{(s)^{\mathrm{T}}} \boldsymbol{\lambda}$ of Eq. (17). The interface connection forces $\boldsymbol{\lambda}$ have to be determined to satisfy the interface compatibility condition between the substructures. Like the interface compatibility condition in Eq. (15), this condition is written in state-space format as

$$\sum_{s=1}^{N} \boldsymbol{B}_{\mathrm{ss}}^{(s)} \boldsymbol{z}^{(s)} = \sum_{s=1}^{N} \left(\begin{bmatrix} \boldsymbol{B}_{\mathrm{ss},u}^{(s)} & \boldsymbol{B}_{\mathrm{ss},v}^{(s)} \end{bmatrix} \begin{bmatrix} \boldsymbol{u}^{(s)} \\ \boldsymbol{v}^{(s)} \end{bmatrix} \right) = \boldsymbol{0} \tag{46}$$

with the state-space substructure constraint matrix $\boldsymbol{B}_{\mathrm{ss}}^{(s)}$ of each substructure s. In Eq. (46), matrix $\boldsymbol{B}_{\mathrm{ss}}^{(s)}$ is split into two parts: one part $\boldsymbol{B}_{\mathrm{ss},u}^{(s)}$ corresponding to the displacements $\boldsymbol{u}^{(s)}$ and into a second part $\boldsymbol{B}_{\mathrm{ss},v}^{(s)}$ corresponding to the velocities $\boldsymbol{v}^{(s)}$ of state-space vector $\boldsymbol{z}^{(s)}$. Comparing the constraint equations (16) and (46), it is concluded that

$$\boldsymbol{B}_{\mathrm{ss},u}^{(s)} = \boldsymbol{B}^{(s)} \qquad \text{and} \qquad \boldsymbol{B}_{\mathrm{ss},v}^{(s)} = \boldsymbol{0}. \tag{47}$$

The static solution $\boldsymbol{z}_{\mathrm{stat}}^{(s)}$ of Eq. (45) is therefore written as

$$\boldsymbol{z}_{\mathrm{stat}}^{(s)} = -\boldsymbol{\mathcal{B}}^{(s)^{-1}} \boldsymbol{B}_{\mathrm{ss}}^{(s)^{\mathrm{T}}} \boldsymbol{\lambda} \tag{48}$$

if $\boldsymbol{\mathcal{B}}^{(s)}$ is invertible. If a substructure has $n_r^{(s)}$ rigid body modes $\boldsymbol{r}_{\mathrm{ss},j}^{(s)}$, $j = 1, \ldots, n_r^{(s)}$, those rigid body modes have to be added to the static solution of Eq. (48). Matrix $\boldsymbol{R}_{\mathrm{ss}}^{(s)}$ contains all of the substructure's regular state-space rigid body modes $\boldsymbol{R}_{\mathrm{ss,reg}}$ and generalized state-space rigid body modes $\boldsymbol{R}_{\mathrm{ss,gen}}$. In this case, matrix $\boldsymbol{\mathcal{B}}^{(s)}$ is singular and the generalized inverse $\boldsymbol{\mathcal{B}}^{(s)^+}$ has to be used instead of $\boldsymbol{\mathcal{B}}^{(s)^{-1}}$. The state-space elastic flexibility matrix $\boldsymbol{G}_{\mathrm{ss}}^{(s)}$ in inertia-relief format is computed from any generalized inverse $\boldsymbol{\mathcal{B}}^{(s)^+}$ by projecting out the rigid body modes $\boldsymbol{R}_{\mathrm{ss}}^{(s)}$ using the inertia-relief projection matrix $\boldsymbol{P}_{\mathrm{ss}}^{(s)}$, which is defined as [25, 39]

$$\boldsymbol{P}_{\mathrm{ss}}^{(s)} = \boldsymbol{I}^{(s)} - \boldsymbol{\mathcal{A}}^{(s)} \boldsymbol{R}_{\mathrm{ss}}^{(s)} \boldsymbol{\mathcal{A}}_{n_r}^{(s)^{-1}} \boldsymbol{R}_{\mathrm{ss}}^{(s)^{\mathrm{T}}} \qquad \text{with} \qquad \boldsymbol{\mathcal{A}}_{n_r}^{(s)} = \boldsymbol{R}_{\mathrm{ss}}^{(s)^{\mathrm{T}}} \boldsymbol{\mathcal{A}}^{(s)} \boldsymbol{R}_{\mathrm{ss}}^{(s)}. \tag{49}$$

Note that $\boldsymbol{\mathcal{A}}_{n_r}^{(s)}$ is not necessarily diagonal [39]. Like the elastic flexibility matrix $\boldsymbol{G}^{(s)}$ in Eq. (25), the state-space elastic flexibility matrix $\boldsymbol{G}_{\mathrm{ss}}^{(s)}$ in inertia-relief format is

$$\boldsymbol{G}_{\mathrm{ss}}^{(s)} = \boldsymbol{P}_{\mathrm{ss}}^{(s)^{\mathrm{T}}} \boldsymbol{\mathcal{B}}^{(s)^+} \boldsymbol{P}_{\mathrm{ss}}^{(s)}. \tag{50}$$

If a substructure has rigid body DOFs, the static solution $\boldsymbol{z}_{\mathrm{stat}}^{(s)}$ is

$$\boldsymbol{z}_{\mathrm{stat}}^{(s)} = -\boldsymbol{G}_{\mathrm{ss}}^{(s)} \boldsymbol{B}_{\mathrm{ss}}^{(s)^{\mathrm{T}}} \boldsymbol{\lambda} + \boldsymbol{R}_{\mathrm{ss}}^{(s)} \boldsymbol{\alpha}^{(s)}. \tag{51}$$

5.3. Substructure approximation and dual assembly

Using the expressions for $z_{\mathrm{stat}}^{(s)}$ in Eq. (51) and for $z_{\mathrm{dyn}}^{(s)}$ in Eq. (43), an approximation of the state-space vector $z^{(s)}$ in Eq. (38) is given by

$$z^{(s)} \approx -G_{\mathrm{ss}}^{(s)} B_{\mathrm{ss}}^{(s)\mathrm{T}} \lambda + R_{\mathrm{ss}}^{(s)} \alpha^{(s)} + \tilde{\Theta}_{\mathrm{ss}}^{(s)} p^{(s)}. \tag{52}$$

Since a part of the subspace spanned by $\tilde{\Theta}_{\mathrm{ss}}^{(s)}$ is already included in $G_{\mathrm{ss}}^{(s)}$, the state-space residual flexibility matrix $G_{\mathrm{ss,res}}^{(s)}$ can be used instead of the state-space flexibility matrix $G_{\mathrm{ss}}^{(s)}$. The state-space residual flexibility matrix $G_{\mathrm{ss,res}}^{(s)}$ is defined by

$$G_{\mathrm{ss,res}}^{(s)} = G_{\mathrm{ss}}^{(s)} - \sum_{j=1}^{n_\theta^{(s)}} \frac{\theta_{\mathrm{ss},j}^{(s)} \theta_{\mathrm{ss},j}^{(s)\mathrm{T}}}{\sigma_j^{(s)}}. \tag{53}$$

As a result, the approximation of one substructure's state-space vector $z^{(s)}$ is

$$z^{(s)} \approx -G_{\mathrm{ss,res}}^{(s)} B_{\mathrm{ss}}^{(s)\mathrm{T}} \lambda + R_{\mathrm{ss}}^{(s)} \alpha^{(s)} + \tilde{\Theta}_{\mathrm{ss}}^{(s)} p^{(s)} = \begin{bmatrix} R_{\mathrm{ss}}^{(s)} & \tilde{\Theta}_{\mathrm{ss}}^{(s)} & -G_{\mathrm{ss,res}}^{(s)} B_{\mathrm{ss}}^{(s)\mathrm{T}} \end{bmatrix} \begin{bmatrix} \alpha^{(s)} \\ p^{(s)} \\ \lambda \end{bmatrix}. \tag{54}$$

Using the approximation of Eq. (54) for the state-space vectors $z^{(s)}$ of all N substructures, the global partitioned, concatenated state-space vector

$$z_{\mathrm{bd}} = \begin{bmatrix} z^{(1)} \\ \vdots \\ z^{(N)} \end{bmatrix} \tag{55}$$

and all Lagrange multipliers λ are approximated by

$$\begin{bmatrix} z_{\mathrm{bd}} \\ \lambda \end{bmatrix} \approx \underbrace{\begin{bmatrix} R_{\mathrm{ss}}^{(1)} & \tilde{\Theta}_{\mathrm{ss}}^{(1)} & & 0 & 0 & -G_{\mathrm{ss,res}}^{(1)} B_{\mathrm{ss}}^{(1)\mathrm{T}} \\ & & \ddots & \ddots & & \vdots \\ 0 & 0 & & R_{\mathrm{ss}}^{(N)} & \tilde{\Theta}_{\mathrm{ss}}^{(N)} & -G_{\mathrm{ss,res}}^{(N)} B_{\mathrm{ss}}^{(N)\mathrm{T}} \\ 0 & 0 & & 0 & 0 & I \end{bmatrix}}_{T_{\mathrm{ss,DCB}}} \begin{bmatrix} \alpha^{(1)} \\ p^{(1)} \\ \vdots \\ \alpha^{(N)} \\ p^{(N)} \\ \lambda \end{bmatrix}. \tag{56}$$

Matrix $T_{\mathrm{ss,DCB}}$ is the dual Craig-Bampton reduction matrix in state-space format. The approximation of the dual assembled system's dynamic equations in state-space format is

$$\mathcal{A}_{\mathrm{DCB}} \begin{bmatrix} \dot{\alpha}^{(1)} \\ \dot{p}^{(1)} \\ \vdots \\ \dot{\alpha}^{(N)} \\ \dot{p}^{(N)} \\ \dot{\lambda} \end{bmatrix} + \mathcal{B}_{\mathrm{DCB}} \begin{bmatrix} \alpha^{(1)} \\ p^{(1)} \\ \vdots \\ \alpha^{(N)} \\ p^{(N)} \\ \lambda \end{bmatrix} = \mathcal{F}_{\mathrm{DCB}} \tag{57}$$

with

$$\mathcal{A}_{\mathrm{DCB}} = T_{\mathrm{ss,DCB}}^{\mathrm{T}} \begin{bmatrix} \mathcal{A}_{\mathrm{bd}} & 0 \\ 0 & 0 \end{bmatrix} T_{\mathrm{ss,DCB}}, \quad \mathcal{B}_{\mathrm{DCB}} = T_{\mathrm{ss,DCB}}^{\mathrm{T}} \begin{bmatrix} \mathcal{B}_{\mathrm{bd}} & B_{\mathrm{ss}}^{\mathrm{T}} \\ B_{\mathrm{ss}} & 0 \end{bmatrix} T_{\mathrm{ss,DCB}}, \quad \mathcal{F}_{\mathrm{DCB}} = T_{\mathrm{ss,DCB}}^{\mathrm{T}} \begin{bmatrix} \mathcal{F}_{\mathrm{bd}} \\ 0 \end{bmatrix}. \tag{58}$$

The block-diagonal matrices $\mathcal{A}_{\mathrm{bd}}$ and $\mathcal{B}_{\mathrm{bd}}$, the state-space constraint matrix B_{ss} and the external force vector $\mathcal{F}_{\mathrm{bd}}$ in Eq. (58) are thereby defined as

$$
\mathcal{A}_{\mathrm{bd}} = \begin{bmatrix} \mathcal{A}^{(1)} & & 0 \\ & \ddots & \\ 0 & & \mathcal{A}^{(N)} \end{bmatrix}, \quad \mathcal{B}_{\mathrm{bd}} = \begin{bmatrix} \mathcal{B}^{(1)} & & 0 \\ & \ddots & \\ 0 & & \mathcal{B}^{(N)} \end{bmatrix}, \quad B_{\mathrm{ss}} = \begin{bmatrix} B_{\mathrm{ss}}^{(1)} & \cdots & B_{\mathrm{ss}}^{(N)} \end{bmatrix}, \quad \mathcal{F}_{\mathrm{bd}} = \begin{bmatrix} \mathcal{F}^{(1)} \\ \vdots \\ \mathcal{F}^{(N)} \end{bmatrix}.
$$
(59)

The dual Craig-Bampton reduced system in Eq. (57) has the final size of $n_{\mathrm{DCB}} = \sum_{s=1}^{N} n_r^{(s)} + \sum_{s=1}^{N} n_\theta^{(s)} + n_\lambda$ states with $n_r^{(s)}$ state-space rigid body modes of substructure s, with $n_\theta^{(s)}$ kept free interface normal modes of substructure s, and with the total number n_λ of all Lagrange multipliers.

Note that the dual Craig-Bampton approach for damped systems can lead to eigenvalues with positive real parts and corresponding spurious modes just as the original formulation of the dual Craig-Bampton method [5] for the undamped case does (see Section 4.2). This does not influence the very good approximation accuracy of the eigenvalues and eigenvectors of systems with general viscous damping, which is demonstrated in the following section.

6. Application example

The bending vibration (no axial deformation) of a beam structure is considered for the numerical evaluation of the proposed substructure reduction method. This example has already been used in [25]. As illustrated in Figure 1, the beam structure is 1.8 m long, consists of 18 Euler-Bernoulli beam elements, and is clamped at the left end and divided into substructure 1 (10 beam elements, length 1.0 m) and substructure 2 (8 beam elements, length 0.8 m). A localized viscous damper is attached to each of the two substructures. In this example, the assembled beam structure's damping matrix C does not satisfy the
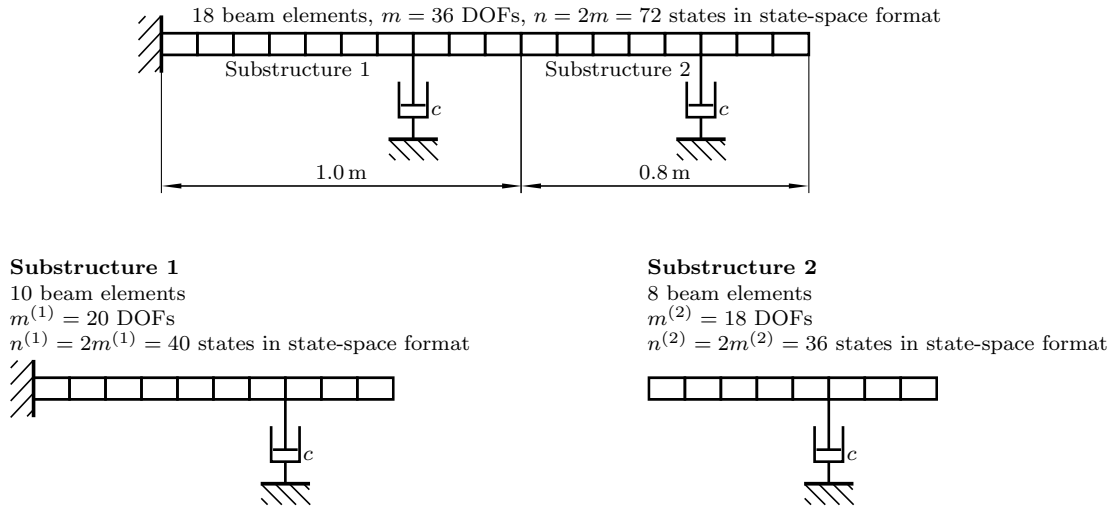
Figure 1: Clamped beam consisting of 18 finite elements with two localized dampers divided into 2 substructures [25]. The clamped beam structure is modeled by 18 Euler-Bernoulli beam elements (cross-section $9.0 \times 10^{-4}\,\mathrm{m}^2$, moment of inertia $7.0 \times 10^{-8}\,\mathrm{m}^4$, Young's modulus $2.1 \times 10^{11}\,\mathrm{N\,m^{-2}}$, density $7.8 \times 10^3\,\mathrm{kg\,m^{-3}}$) and has $m = 36$ DOFs. The length of substructure 1 is 1.0 m, the length of substructure 2 is 0.8 m and the damper constant c is $1.0 \times 10^4\,\mathrm{N\,s\,m^{-1}}$.

condition of Eq. (7). Decoupling is therefore not possible using classical modal analysis. Moreover, rigid body movement is possible for substructure 2. Substructure 2 has $m_r^{(2)} = 2$ physical rigid body modes (translational rigid body movement $r_{\mathrm{trans}}^{(2)}$ and rotatory rigid body movement $r_{\mathrm{rot}}^{(2)}$). In this example, this

leads to one single zero eigenvalue (translation mode) and one zero eigenvalue with multiplicity two (rotation mode) for substructure 2 in state-space form. This is due to the fact that the translational rigid body movement $r_{\text{trans}}^{(2)}$ is damped by the localized damper c (i.e., a damping force will act if substructure 2 moves in the translation mode), but the rotational rigid body movement $r_{\text{rot}}^{(2)}$ is not damped (i.e., no damping force will be caused if substructure 2 moves in the rotation mode). The physical translational rigid body $r_{\text{trans}}^{(2)}$ mode will activate the damper and thus $C^{(2)}r_{\text{trans}}^{(2)} \neq 0$. Therefore, according to the theory ($C^{(2)}r_{\text{trans}}^{(2)} \neq 0$, for details see Appendix B), the physical translational rigid body $r_{\text{trans}}^{(2)}$ is not defective and has a multiplicity one for the state-space eigenvalue problem. Thus, only one regular state-space translational rigid body mode $r_{\text{ss,trans,reg}}^{(2)}$ is associated to the physical translational rigid body mode $r_{\text{trans}}^{(2)}$. The second physical rigid body $r_{\text{rot}}^{(2)}$ represents a rotation around the damper and therefore $C^{(2)}r_{\text{rot}}^{(2)} = 0$, i.e., the physical rigid body $r_{\text{rot}}^{(2)}$ does not activate the damper. According to the theory ($C^{(2)}r_{\text{rot}}^{(2)} = 0$), both a regular state-space rotational rigid body mode $r_{\text{ss,rot,reg}}^{(2)}$ and a generalized state-space rotational rigid body mode $r_{\text{ss,rot,gen}}^{(2)}$ are associated to the physical rotational rigid body mode $r_{\text{rot}}^{(2)}$. Hence, one regular state-space rigid body mode corresponds to the physical translational movement $r_{\text{trans}}^{(2)}$, and both a regular state-space rigid body mode and a generalized state-space rigid body mode correspond to the physical rotational movement $r_{\text{rot}}^{(2)}$.

From a mechanical point of view, the mathematical relations of Section 5 and Appendix B concerning state-space rigid body modes can be interpreted as follows: If a damping force acts when a substructure moves in a physical rigid body mode $r_j^{(s)}$ (situation $C^{(s)}r_j^{(s)} \neq 0$), only a regular state-space rigid body mode $r_{\text{ss},j,\text{reg}}^{(s)}$ is associated to the physical rigid body mode $r_j^{(s)}$. On the other hand, if no damping force acts when the substructure moves in a physical rigid body mode $r_j^{(s)}$ (situation $C^{(s)}r_j^{(s)} = 0$), one regular state-space rigid body mode $r_{\text{ss},j,\text{reg}}^{(s)}$ and one generalized state-space rigid body mode $r_{\text{ss},j,\text{gen}}^{(s)}$ is associated to the physical rigid body mode $r_j^{(s)}$.

6.1. Eigenvalues of unreduced system

Figure 2 depicts all 72 eigenvalues in the complex plane for the coupled unreduced system. Eigenvalues of the coupled unreduced (full) system will be called σ_{full}. It can be seen that the system has a lot of complex conjugate eigenvalue pairs. In total, there are 68 complex eigenvalues with imaginary parts, i.e., 34 underdamped complex conjugate eigenvalue pairs. The complex conjugate eigenvalue pairs have imaginary parts $|\Im(\sigma_{\text{full}})| > 650\,\text{rad}\,\text{s}^{-1}$ leading to underdamped modes. In contrast, there are exactly four eigenvalues without imaginary part [25]. These four real eigenvalues indicate very high damping leading to overdamped modes [6].

6.2. Approximation of eigenvalues

The beam structure's lowest eigenvalues are approximated by the proposed dual Craig-Bampton formulation for damped systems. Eigenvalues of the reduced system will be called σ_{red}. Therefore, the eigenvalue problem

$$(\sigma_{\text{red},j}\mathcal{A}_{\text{DCB}} + \mathcal{B}_{\text{DCB}})\,\psi_{\text{red},j} = 0 \tag{60}$$

with the dual Craig-Bampton reduced matrices $\mathcal{A}_{\text{DCB}}$ and $\mathcal{B}_{\text{DCB}}$ of Eq. (58) is solved for the eigenvalues. For comparison, they will also be approximated by a classical Craig-Bampton method for damped systems. The classical Craig-Bampton method uses complex component fixed interface normal modes and constraint modes. The Craig-Bampton formulation for damped systems from [24] is used for the comparison.

For the time being, we keep the complex free interface normal modes $\theta_{\text{ss},j}^{(1)}$ corresponding to the $n_\theta^{(1)} = 20$ eigenvalues with lowest absolute magnitude for substructure 1 (two of the $n_\theta^{(1)} = 20$ eigenvalues are overdamped eigenvalues and the other 18 eigenvalues are 9 complex conjugate pairs) and the complex free interface normal modes $\theta_{\text{ss},j}^{(2)}$ corresponding to the $n_\theta^{(2)} = 19$ eigenvalues with lowest absolute magnitude for substructure 2 (one of the $n_\theta^{(2)} = 19$ eigenvalues is an overdamped eigenvalue and the other 18 eigenvalues

13
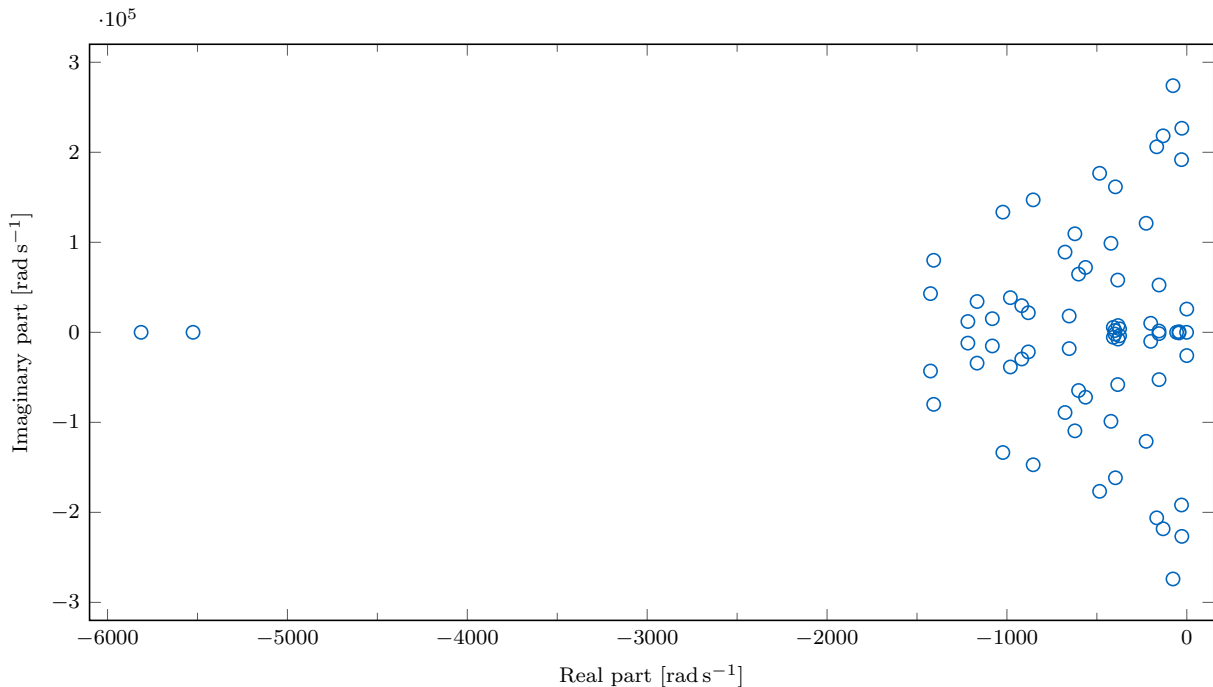
Figure 2: All eigenvalues σ_{full} of the coupled unreduced system of Figure 1 in the complex plane.

are 9 complex conjugate pairs). Substructure 1 is clamped, but substructure 2 has $n_r^{(2)} = 3$ state-space rigid body modes. The substructures are coupled by $n_\lambda = 2$ Lagrange multipliers corresponding to the two interface states. After coupling, the reduced system has $n_{\text{DCB}} = 44$ states according to Eq. (57). The eigenvalues σ_{red} of the dual Craig-Bampton reduced system are computed as written in Eq. (60). Figure 3 shows the approximated eigenvalues σ_{red} with an absolute value of the imaginary part $|\Im(\sigma_{\text{red}})| \leq 80\,000\,\text{rad}\,\text{s}^{-1}$. Eigenvalues σ_{red} with $|\Im(\sigma_{\text{red}})| \leq 50\,000\,\text{rad}\,\text{s}^{-1}$ approximate the true eigenvalues σ_{full} of the full system very accurately. Admittedly, it is difficult to identify in Figure 3 which true eigenvalues σ_{full} are approximated by which eigenvalues σ_{red} if $|\Im(\sigma_{\text{red}})| > 50\,000\,\text{rad}\,\text{s}^{-1}$. The approximation accuracy in the low frequency range (i.e., for eigenvalues σ_{red} with small imaginary parts) is nevertheless very good and Figure 4 gives a zoom plot of Figure 3 to visualize this. To investigate the approximation accuracy quantitatively, the relative errors of approximated eigenvalues are considered in Section 6.3.

Eigenvalues obtained from a Craig-Bampton approximation are depicted in Figure 3 and 4 in addition to those approximated using the proposed dual Craig-Bampton method. The Craig-Bampton approximation keeps complex fixed interface normal modes corresponding to the 20 eigenvalues with lowest absolute magnitude for substructure 1, complex fixed interface normal modes corresponding to the 20 eigenvalues with lowest absolute magnitude for substructure 2, and four constraint modes for each substructure since the two substructures share four states. After coupling, the reduced system has $n_{\text{CB}} = 44$ states, which is equal to the number of $n_{\text{DCB}} = 44$ states of the dual Craig-Bampton reduced system. In Figure 3, it can be seen that the dual Craig-Bampton method gives a considerably better approximation of the true eigenvalues than the Craig-Bampton method does with the same number of states of the reduced system. Figure 4 gives a zoom plot of Figure 3 in the frequency band $|\Im(\sigma_{\text{red}})| \leq 12\,500\,\text{rad}\,\text{s}^{-1}$, i.e., in the frequency band corresponding to eigenvalues with small imaginary parts. Both methods approximate the eigenvalues in the low frequency range accurately. Nevertheless, the dual Craig-Bampton method gives an even better approximation than the Craig-Bampton method. The approximated eigenvalues obtained using the dual Craig-Bampton method coincide with the true eigenvalues much better than the eigenvalues obtained using the Craig-Bampton method.

14
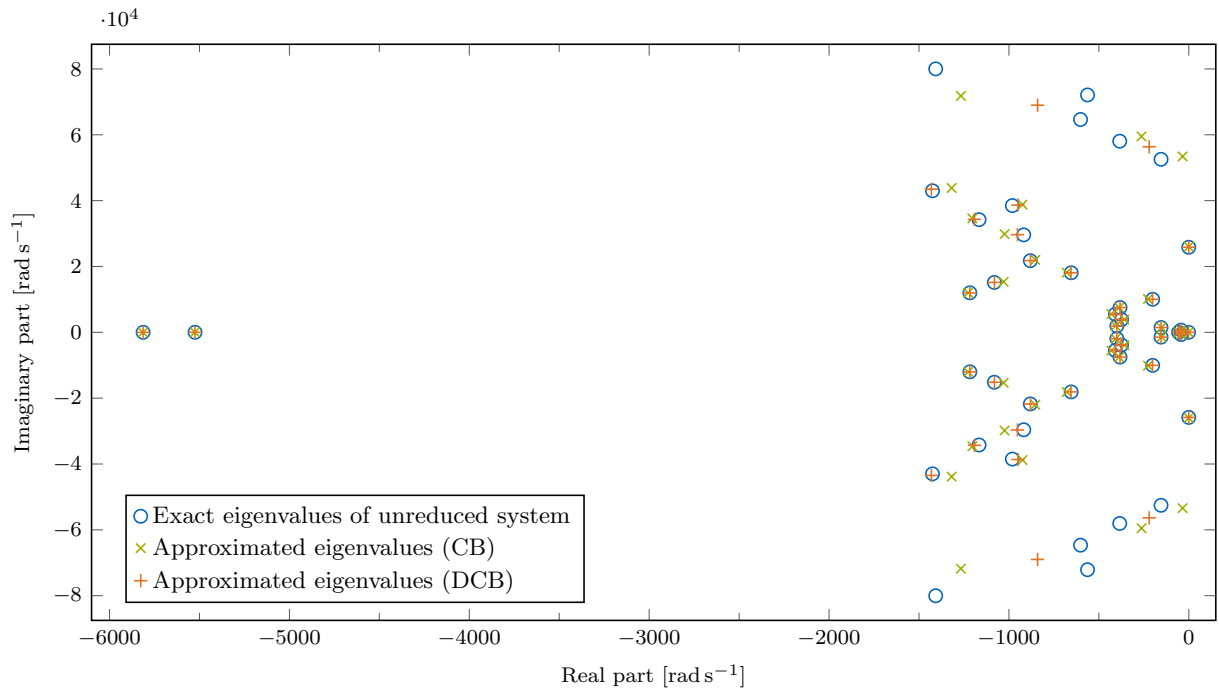
Figure 3: Eigenvalues σ_{full} of the coupled unreduced system and eigenvalues σ_{red} of the reduced system in the complex plane. The eigenvalues are approximated on the one hand with a classical Craig-Bampton (CB) method for damped systems [24] and on the other hand with the proposed dual Craig-Bampton (DCB) method for damped systems. The number $n_{\text{CB}} = n_{\text{DCB}} = 44$ of states of the reduced systems are equal.
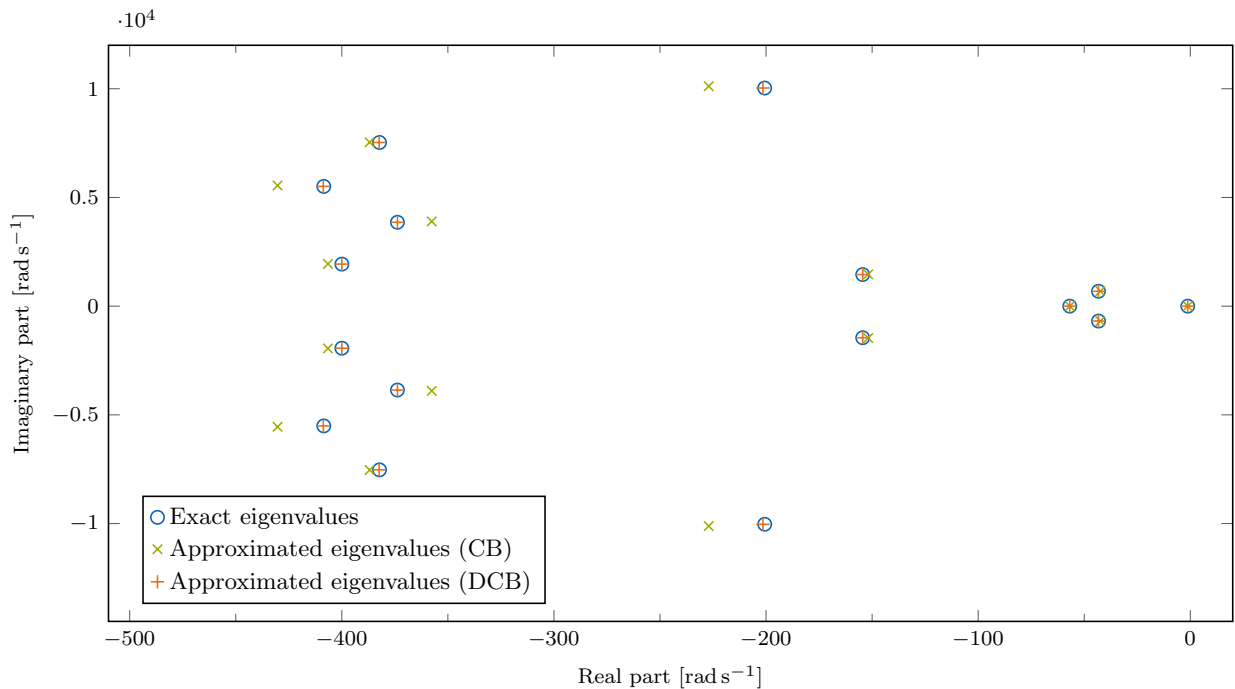
Figure 4: Zoom plot of Figure 3 in the eigenvalue band $-500\,\text{rad}\,\text{s}^{-1} \leq \Re(\sigma_{\text{red}}) \leq 0\,\text{rad}\,\text{s}^{-1}$ and $|\Im(\sigma_{\text{red}})| \leq 12\,500\,\text{rad}\,\text{s}^{-1}$.

15

6.3. Relative errors of approximated eigenvalues

To highlight the very good approximation accuracy of the suggested dual Craig-Bampton approach, the relative errors $\varepsilon_{\text{rel},\Re}$ of the eigenvalues' real parts and relative errors $\varepsilon_{\text{rel},\Im}$ of the eigenvalues' imaginary parts are now considered. The relative errors $\varepsilon_{\text{rel},\Re,j}$ of the real parts and the relative errors $\varepsilon_{\text{rel},\Im,j}$ of the imaginary parts of the j-th eigenvalue are computed according to

$$\varepsilon_{\text{rel},\Re,j} = \frac{|\Re(\sigma_{\text{red},j}) - \Re(\sigma_{\text{full},j})|}{\Re(\sigma_{\text{full},j})} \qquad \text{and} \qquad \varepsilon_{\text{rel},\Im,j} = \frac{|\Im(\sigma_{\text{red},j}) - \Im(\sigma_{\text{full},j})|}{\Im(\sigma_{\text{full},j})}. \tag{61}$$

In Eq. (61), $\sigma_{\text{full},j}$ is the j-th eigenvalue of the full (unreduced and coupled) system and $\sigma_{\text{red},j}$ is the j-th eigenvalue of the reduced system. Figure 5 shows the relative errors $\varepsilon_{\text{rel},\Re}$ of the eigenvalues' real parts (Figure 5a) and the relative errors $\varepsilon_{\text{rel},\Im}$ of the eigenvalues' imaginary parts (Figure 5b) for the considered system. The number of states of the reduced systems, $n_{\text{CB}} = n_{\text{DCB}} = 44$, is the same for the Craig-Bampton and the dual Craig-Bampton reduction. When the relative error $\varepsilon_{\text{rel},\Im}$ of the imaginary part of an eigenvalue σ_{red} is missing, it means that the imaginary part $\Im(\sigma_{\text{red}})$ of the eigenvalue is zero. On the other
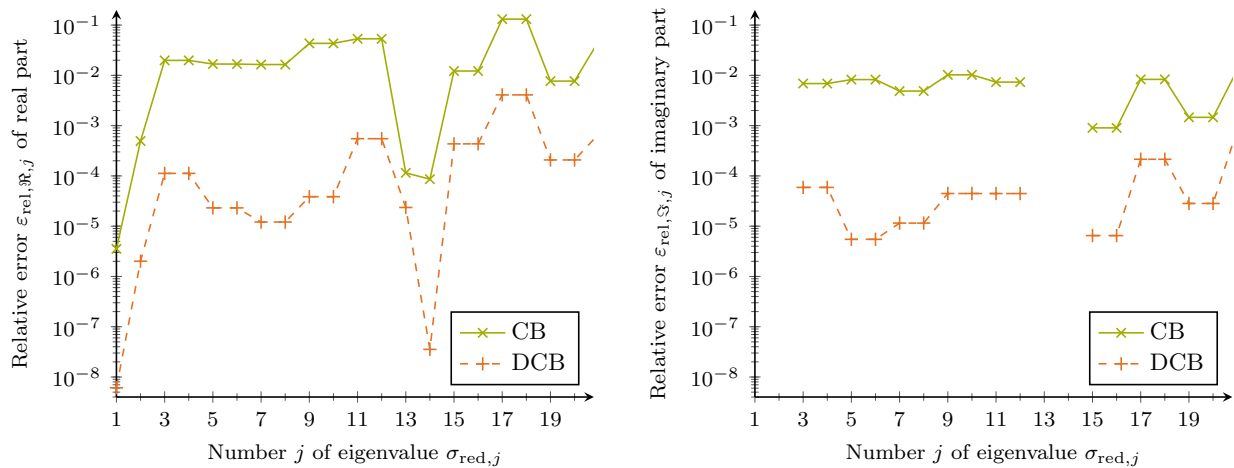
(a) Relative error $\varepsilon_{\text{rel},\Re,j}$ of the real part of eigenvalue $\sigma_{\text{red},j}$.

(b) Relative error $\varepsilon_{\text{rel},\Im,j}$ of the imaginary part of eigenvalue $\sigma_{\text{red},j}$.

Figure 5: Relative error of real and imaginary parts of eigenvalue σ_{red}. The lowest 20 eigenvalues are approximated using the Craig-Bampton method (CB) and the dual Craig-Bampton method (DCB). The number of states of the reduced systems, $n_{\text{CB}} = n_{\text{DCB}} = 44$, is the same. When the relative error $\varepsilon_{\text{rel},\Im}$ of the imaginary part of an eigenvalue σ_{red} is missing, it means that the imaginary part $\Im(\sigma_{\text{red}})$ of the eigenvalue is zero.

hand, the real eigenvalues (eigenvalues 1, 2, 13, and 14) with no imaginary parts are approximated very well. Generally speaking, the imaginary parts are approximated slightly better than the corresponding real parts. But if real eigenvalues occur (i.e., with no imaginary part), these real eigenvalues are also approximated accurately. This is a very important property since real eigenvalues indicate very high damping leading to overdamped modes [6], which contribute significantly to the dynamical behavior of damped systems.

Comparing both methods, the accuracy of the dual Craig-Bampton approximation is around two orders of magnitude better than that of the Craig-Bampton approximation in the low eigenvalue range. Both methods lead to a reduced system with the same number of states. This example indicates that the proposed dual Craig-Bampton approach exhibits very good approximation accuracy compared to the classical Craig-Bampton approach.

In addition, we want to examine the approximation accuracy of the proposed method for eigenvectors. Therefore, eigenvector $\boldsymbol{\psi}_{\text{red},j}$ corresponding to j-th eigenvalue $\sigma_{\text{red},j}$ of the dual Craig-Bampton reduced system in Eq. (60) is compared to the eigenvector $\boldsymbol{\psi}_{\text{full},j}$ of the unreduced (full) system. We consider the

16

modal assurance criterion

$$MAC_j = \frac{\left| \boldsymbol{\psi}_{\text{full},j}^{\text{H}} \, \boldsymbol{\psi}_{\text{red},j} \right|^2}{\boldsymbol{\psi}_{\text{full},j}^{\text{H}} \, \boldsymbol{\psi}_{\text{full},j} \, \boldsymbol{\psi}_{\text{red},j}^{\text{H}} \, \boldsymbol{\psi}_{\text{red},j}} \tag{62}$$

between the j-th eigenvector $\boldsymbol{\psi}_{\text{full},j}$ of the full system and the j-th eigenvector $\boldsymbol{\psi}_{\text{red},j}$ of the reduced system [40, 41]. Thereby, $(\bullet)^{\text{H}}$ represents the Hermitian transpose (also called conjugate transpose), but not simply the transpose $(\bullet)^{\text{T}}$. The modal assurance criterion is a scalar value and can take values between 0, which is an indication that the vectors are not consistent, and 1, which is an indication that the modal vectors are consistent [41]. Table 1 shows the modal assurance criterion MAC_j for the eigenvectors corre-

j	MAC_j	j	MAC_j
1	0.9995	11	0.9775
2	0.9980	12	0.9775
3	0.9985	13	0.9897
4	0.9985	14	1.0000
5	0.9947	15	0.9956
6	0.9947	16	0.9956
7	0.9962	17	0.9567
8	0.9962	18	0.9567
9	0.9809	19	0.9971
10	0.9809	20	0.9971

Table 1: Modal assurance criterion MAC_j between j-th eigenvector of the full system and j-th eigenvector of the dual Craig-Bampton reduced system with $n_{\text{DCB}} = 44$ states.

sponding to the 20 lowest eigenvalues of the dual Craig-Bampton reduced system with $n_{\text{DCB}} = 44$ states (for relative errors of the eigenvalues see Figure 5). The MAC_j values are very close to 1 indicating consistent correspondence between the eigenvectors of the full and the reduced system. Especially, the eigenvectors corresponding to the real eigenvalues (eigenvalues 1, 2, 13, and 14) are approximated very well. This demonstrates that the proposed dual Craig-Bampton approach exhibits also very good approximation accuracy for eigenvectors of damped systems.

6.4. Keeping different numbers of normal modes per substructure

6.4.1. Dual Craig-Bampton approach

Similar graphs depicting the relative errors $\varepsilon_{\text{rel},\Re}$ and $\varepsilon_{\text{rel},\Im}$ as in Figure 5 are obtained using different numbers of normal modes per substructure for the two methods. For the dual Craig-Bampton approximation in Figure 5, we kept $n_\theta^{(1)} = 20$ complex free interface normal modes for substructure 1 and $n_\theta^{(2)} = 19$ complex free interface normal modes for substructure 2. The $n_r^{(2)} = 3$ state-space rigid body modes of substructure 2 are retained in the reduction basis in any case. Figure 6 shows the relative errors when the numbers of kept complex normal modes $n_\theta^{(1)}$ and $n_\theta^{(2)}$ are varied for the dual Craig-Bampton approximation. The real eigenvalues (eigenvalues 1, 2, 13, and 14) with no imaginary parts are again approximated very well. This is also valid if only $n_\theta^{(1)} = 8$ and $n_\theta^{(2)} = 7$ complex free interface normal modes are kept, which results in a reduced system of size $n_{\text{DCB}} = 20$.

On the other hand, the corresponding imaginary part is approximated more accurately than the real part if the eigenvalues are complex. Generally speaking, the imaginary parts are approximated better than the corresponding real parts, which was also observed by de Kraker and van Campen for the Rubin method in [25].
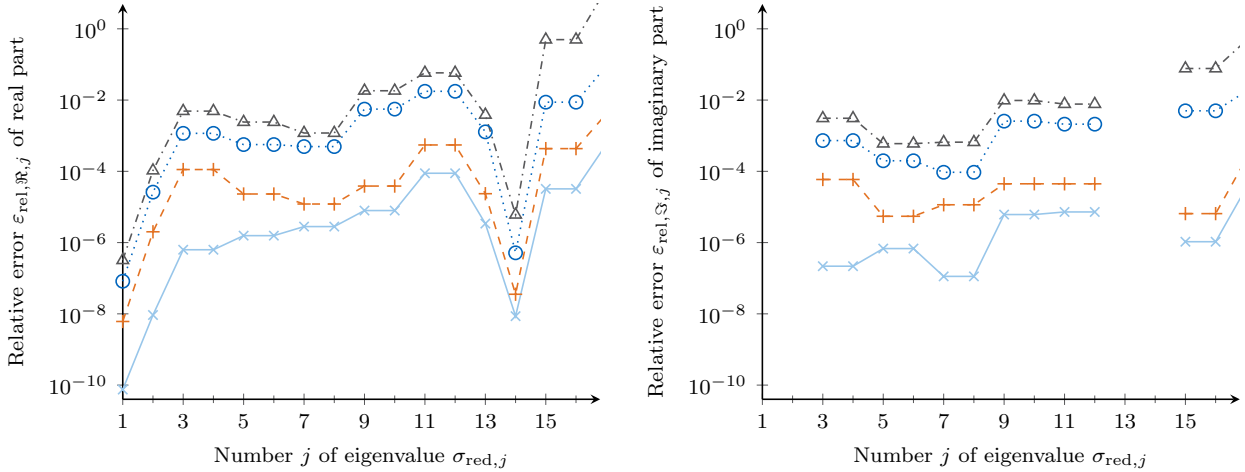
(a) Relative error $\varepsilon_{\mathrm{rel},\Re,j}$ of the real part of eigenvalue j.

(b) Relative error $\varepsilon_{\mathrm{rel},\Im,j}$ of the imaginary part of eigenvalue j.

Figure 6: Relative error of real and imaginary parts of eigenvalue σ_{red}. The lowest 16 eigenvalues are approximated using the dual Craig-Bampton method (DCB). The number $n_\theta^{(1)}$ of kept complex free interface normal modes for substructure 1 and the number $n_\theta^{(2)}$ of kept complex free interface normal modes for substructure 2 is varied. The $n_r^{(2)} = 3$ rigid body modes of substructure 2 are retained in the reduction basis in any case. When the relative error $\varepsilon_{\mathrm{rel},\Im}$ of the imaginary part of an eigenvalue σ is missing, it means that the imaginary part $\Im(\sigma)$ of the eigenvalue is zero.

6.4.2. Comparison of Craig-Bampton and dual Craig-Bampton approach for similar accuracy

Finally, we want to illustrate the performance of the proposed dual Craig-Bampton approach compared to the classical Craig-Bampton formulation. Therefore, we aim at approximating the eigenvalues using the minimal number of normal modes per substructure necessary to reach a certain maximum relative error for the real and imaginary parts of eigenvalues according to Eq. (61).

We chose to approximate the lowest 14 eigenvalues, i.e., the minimum number including all overdamped eigenvalues, and set the threshold for the maximum relative error arbitrarily to 5%. By trial and error, we find that to reach

$$\max\left(\varepsilon_{\mathrm{rel},\Re,j}\right) < 5\% \qquad \text{and} \qquad \max\left(\varepsilon_{\mathrm{rel},\Im,j}\right) < 5\% \qquad \text{for} \qquad j = 1, \ldots, 14, \qquad (63)$$

we need to keep 22 complex fixed interface normal modes for substructure 1 and 20 complex fixed interface normal modes for substructure 2 for the Craig-Bampton approach, resulting in a reduced system with $n_{\mathrm{CB}} = 46$ states. To reach the maximum relative errors in Eq. (63) with the proposed dual Craig-Bampton approach, we have to keep $n_\theta^{(1)} = 10$ complex free interface normal modes for substructure 1 and $n_\theta^{(2)} = 9$ complex free interface normal modes for substructure 2. Then, the dual Craig-Bampton reduced system has only $n_{\mathrm{DCB}} = 24$ states. Figure 7 shows the relative errors of real and imaginary parts for both approximations. For this example, the relative errors of the real parts of eigenvalues 11 and 12 are the critical errors for both methods. The real eigenvalues (eigenvalues 1, 2, 13, and 14) with no imaginary parts are approximated very well by both methods.

Comparing both methods, the size $n_{\mathrm{DCB}} = 24$ of the reduced system using the dual Craig-Bampton approximation is significantly smaller than the size $n_{\mathrm{CB}} = 46$ of the reduced system using the Craig-Bampton approximation if the error tolerances in Eq. (63) have to be reached. This example demonstrates that the proposed dual Craig-Bampton approach needs to compute less normal modes than the classical Craig-Bampton approach to reach the same accuracy. Less computational effort is necessary and less memory
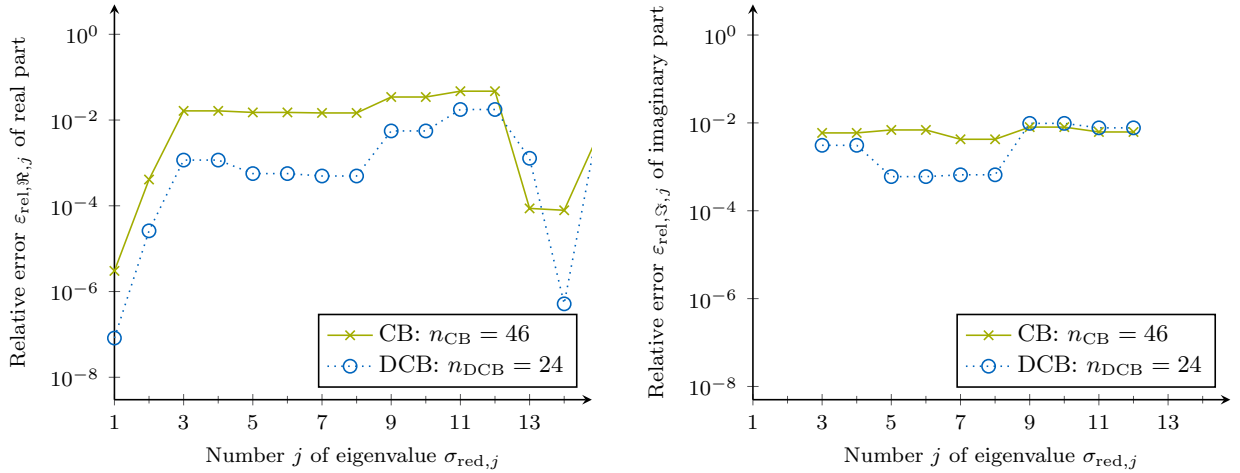
(a) Relative error $\varepsilon_{\mathrm{rel},\Re,j}$ of the real part of eigenvalue $\sigma_{\mathrm{red},j}$.

(b) Relative error $\varepsilon_{\mathrm{rel},\Im,j}$ of the imaginary part of eigenvalue $\sigma_{\mathrm{red},j}$.

Figure 7: Relative error of real and imaginary parts of eigenvalue σ_{red}. The lowest 14 eigenvalues are approximated using the Craig-Bampton method (CB) and the dual Craig-Bampton method (DCB). The number of kept normal modes are chosen such that the maximum relative error of real and imaginary parts of the lowest 14 eigenvalues for the approximation with both methods is 5%. This results in a reduced system with $n_{\mathrm{CB}} = 46$ states for the Craig-Bampton and in a reduced system with $n_{\mathrm{DCB}} = 24$ states for the dual Craig-Bampton method. When the relative error $\varepsilon_{\mathrm{rel},\Im}$ of the imaginary part of an eigenvalue σ_{red} is missing, it means that the imaginary part $\Im(\sigma_{\mathrm{red}})$ of the eigenvalue is zero.

storage is demanded by the dual Craig-Bampton method making this approach more efficient.

7. Conclusions

In this paper, we extended the dual Craig-Bampton method to the case of systems with general viscous damping. In its original form for the undamped case, the reduction matrix is built based on real static modes (rigid body modes and residual flexibility attachment modes) and a number of kept real dynamic modes (free interface normal modes). The extended formulation for incorporating viscous damping is based on a state-space formulation consisting of first-order differential equations. The rigid body mode concept had to be adapted to the possibility of generalized rigid body modes corresponding to multiple zero eigenvalues. Those rigid body modes, complex free interface normal modes, and generalized residual flexibility modes are used to build the reduction basis.

The very good approximation accuracy of eigenvalues and eigenvectors of this dual Craig-Bampton approach for general viscous damping was demonstrated on a beam structure with localized dampers. Resulting in a reduced system with the same number of states, the dual Craig-Bampton approach outperforms the classical Craig-Bampton approach. The approximation accuracy of the eigenvalues is around two orders of magnitude greater showing the potential of this extension of the dual Craig-Bampton method. If a certain error tolerance has to be reached, the dual Craig-Bampton approach needs to keep a significantly smaller number of normal modes than the Craig-Bampton approximation. This results in a smaller reduced system, less computational effort and less memory storage when using the dual Craig-Bampton approximation. Varying the number of kept modes gave rise to monotonically improving approximation accuracy when the number of kept modes is increased. Real eigenvalues without imaginary parts corresponding to overdamped modes are always very well approximated. If the eigenvalues are complex (i.e., they occur in complex conjugate pairs), then the corresponding imaginary parts are usually approximated more accurately than the real parts.

In the future, we want to apply the method to bigger problems. The example used in this paper is very illustrative, allows for comparison to results in the literature and demonstrates all critical points for

19

the application of the suggested methodology, but it is too small for a meaningful comparison in terms of computational time. For this purpose, it is necessary to consider additional numerical examples to further examine the performance of the proposed methods. Nevertheless, it was demonstrated that the proposed method reaches a certain approximation accuracy with much less computational effort than the classical Craig-Bampton approach since significantly less modes have to be computed.

Finally, it is mentioned that the dual Craig-Bampton approach for damped systems can lead to eigenvalues with positive real parts and corresponding spurious modes just as the original formulation of the dual Craig-Bampton method for the undamped case does [5]. This does not influence the very good approximation accuracy of the eigenvalues and eigenvectors of systems with general viscous damping, but it can cause problems in some applications (e.g., time integration, computation of frequency response functions). For the original formulation of the dual Craig-Bampton method, a time integration strategy is investigated in [43] and could also be used for the approach suggested in this contribution. Further research has to be conducted on the spurious eigensolutions obtained by the dual Craig-Bampton approach for damped systems and their effect on subsequent steps after the reduction.

Appendix A. Defective systems and Jordan normal form

Appendix A.1. Standard eigenvalue problem

Consider a square matrix $\boldsymbol{D}$ of dimension $n \times n$ and the corresponding standard eigenvalue problem

$$\sigma_j \boldsymbol{\theta}_j = \boldsymbol{D} \boldsymbol{\theta}_j \quad \Leftrightarrow \quad (\sigma_j \boldsymbol{I} - \boldsymbol{D}) \boldsymbol{\theta}_j = \boldsymbol{0} \tag{A.1}$$

with eigenvalue σ_j and corresponding eigenvector $\boldsymbol{\theta}_j$ for $j = 1, \ldots, n$. The corresponding characteristic polynomial is

$$\det (\sigma_j \boldsymbol{I} - \boldsymbol{D}) = 0. \tag{A.2}$$

The *algebraic multiplicity* of eigenvalue σ_j is its multiplicity as a root of the characteristic polynomial Eq. (A.2). The *geometric multiplicity* of σ_j is the number of linearly independent eigenvectors associated with σ_j. An eigenvalue σ_j with algebraic multiplicity 2 or higher is called a repeated eigenvalue [44]. In contrast, an eigenvalue with algebraic multiplicity 1 is called to be simple [45]. If the algebraic multiplicity of σ_j exceeds its geometric multiplicity, then σ_j is said to be a *defective eigenvalue*. A matrix with a defective eigenvalue is referred to as a *defective matrix* [45]. A defective matrix does not have a linearly independent set of n eigenvectors. Nondefective matrices are also said to be *diagonalizable* [45]. If matrix $\boldsymbol{D}$ is defective, there exists no eigenvector matrix

$$\boldsymbol{\Theta} = \begin{bmatrix} \boldsymbol{\theta}_1 & \boldsymbol{\theta}_2 & \ldots & \boldsymbol{\theta}_n \end{bmatrix} \tag{A.3}$$

such that

$$\boldsymbol{\Theta} \boldsymbol{\Sigma} = \boldsymbol{D} \boldsymbol{\Theta} \tag{A.4}$$

where $\boldsymbol{\Sigma} = \mathrm{diag}\,(\sigma_1, \sigma_2, \ldots, \sigma_n)$ is the diagonal eigenvalue matrix. Nevertheless, it is possible to find a linearly independent set of generalized eigenvectors that transform $\boldsymbol{D}$ into Jordan normal form

$$\boldsymbol{\Theta} \boldsymbol{J} = \boldsymbol{D} \boldsymbol{\Theta} \tag{A.5}$$

with Jordan matrix $\boldsymbol{J}$ [6]. For example, if $\boldsymbol{D}$ is a matrix of dimension 7×7 and has a repeated eigenvalue σ_1 of multiplicity 2 and a repeated eigenvalue σ_2 of multiplicity 3 both with geometric multiplicity of 1 (eigenvalues σ_3 and σ_4 have multiplicity 1), the Jordan matrix $\boldsymbol{J}$ will have the form

$$\boldsymbol{J} = \begin{bmatrix} \sigma_1 & 1 & 0 & 0 & 0 & 0 & 0 \\ 0 & \sigma_1 & 0 & 0 & 0 & 0 & 0 \\ 0 & 0 & \sigma_2 & 1 & 0 & 0 & 0 \\ 0 & 0 & 0 & \sigma_2 & 1 & 0 & 0 \\ 0 & 0 & 0 & 0 & \sigma_2 & 0 & 0 \\ 0 & 0 & 0 & 0 & 0 & \sigma_3 & 0 \\ 0 & 0 & 0 & 0 & 0 & 0 & \sigma_4 \end{bmatrix}. \tag{A.6}$$

Appendix A.2. Generalized eigenvalue problem

The concept of Appendix A.1 can also be applied to the generalized eigenvalue problem[2]

$$-\sigma_j \boldsymbol{A} \boldsymbol{\theta}_{\mathrm{ss},j} = \boldsymbol{B} \boldsymbol{\theta}_{\mathrm{ss},j} \quad \Leftrightarrow \quad (\sigma_j \boldsymbol{A} + \boldsymbol{B}) \boldsymbol{\theta}_{\mathrm{ss},j} = \boldsymbol{0} \tag{A.7}$$

with matrices $\boldsymbol{A}$ and $\boldsymbol{B}$ of dimension $n \times n$, eigenvalue σ_j and corresponding eigenvector $\boldsymbol{\theta}_{\mathrm{ss},j}$ for $j = 1, \ldots, n$. If the eigenvalue problem (A.7) is defective, there exists no eigenvector matrix

$$\boldsymbol{\Theta}_{\mathrm{ss}} = \begin{bmatrix} \boldsymbol{\theta}_{\mathrm{ss},1} & \boldsymbol{\theta}_{\mathrm{ss},2} & \ldots & \boldsymbol{\theta}_{\mathrm{ss},n} \end{bmatrix} \tag{A.8}$$

such that

$$\boldsymbol{A} \boldsymbol{\Theta}_{\mathrm{ss}} \boldsymbol{\Sigma} + \boldsymbol{B} \boldsymbol{\Theta}_{\mathrm{ss}} = \boldsymbol{0} \tag{A.9}$$

where $\boldsymbol{\Sigma} = \mathrm{diag}\,(\sigma_1, \sigma_2, \ldots, \sigma_n)$ is the diagonal eigenvalue matrix. It is possible to find a linearly independent set of generalized eigenvectors that transform $\boldsymbol{A}$ and $\boldsymbol{B}$ into almost-diagonal Jordan normal form

$$\boldsymbol{A} \boldsymbol{\Theta}_{\mathrm{ss}} \boldsymbol{J} + \boldsymbol{B} \boldsymbol{\Theta}_{\mathrm{ss}} = \boldsymbol{0} \tag{A.10}$$

with Jordan matrix $\boldsymbol{J}$, which will have Jordan blocks on the diagonal as for instance in Eq. (A.6). Consider now the part of Eq. (A.10) corresponding to a repeated eigenvalue $\sigma_1 = 0$ of algebraic multiplicity 2 and geometric multiplicity 1:

$$\boldsymbol{A} \begin{bmatrix} \boldsymbol{\theta}_{\mathrm{ss},1,\mathrm{reg}} & \boldsymbol{\theta}_{\mathrm{ss},1,\mathrm{gen}} \end{bmatrix} \begin{bmatrix} 0 & 1 \\ 0 & 0 \end{bmatrix} + \boldsymbol{B} \begin{bmatrix} \boldsymbol{\theta}_{\mathrm{ss},1,\mathrm{reg}} & \boldsymbol{\theta}_{\mathrm{ss},1,\mathrm{gen}} \end{bmatrix} = \begin{bmatrix} \boldsymbol{0} & \boldsymbol{0} \end{bmatrix} \tag{A.11}$$

Vector $\boldsymbol{\theta}_{\mathrm{ss},1,\mathrm{reg}}$ denotes the regular eigenvector corresponding to eigenvalue $\sigma_1 = 0$ that is obtained by solving the eigenvalue problem (A.7). The generalized eigenvector corresponding to eigenvalue $\sigma_1 = 0$ is labeled $\boldsymbol{\theta}_{\mathrm{ss},1,\mathrm{gen}}$. Eq. (A.11) gives two equations:

$$\boldsymbol{B} \boldsymbol{\theta}_{\mathrm{ss},1,\mathrm{reg}} = \boldsymbol{0} \tag{A.12}$$

$$\boldsymbol{A} \boldsymbol{\theta}_{\mathrm{ss},1,\mathrm{reg}} + \boldsymbol{B} \boldsymbol{\theta}_{\mathrm{ss},1,\mathrm{gen}} = \boldsymbol{0} \tag{A.13}$$

Eq. (A.12) reproduces the eigenvalue problem (A.7) with $\sigma_1 = 0$ to obtain the regular eigenvector $\boldsymbol{\theta}_{\mathrm{ss},1,\mathrm{reg}}$. Eq. (A.13) is used to determine the generalized eigenvector $\boldsymbol{\theta}_{\mathrm{ss},1,\mathrm{gen}}$. Both vectors $\boldsymbol{\theta}_{\mathrm{ss},1,\mathrm{reg}}$ and $\boldsymbol{\theta}_{\mathrm{ss},1,\mathrm{gen}}$ can be used to define state-space rigid body modes, which occur if the second-order mechanical system of Eq. (1) with physical rigid body modes is transformed into state-space form.

Appendix B. State-space rigid body modes

Matrix $\boldsymbol{R}$ of dimension $m \times m_r$

$$\boldsymbol{R} = \begin{bmatrix} \boldsymbol{r}_1 & \boldsymbol{r}_2 & \ldots & \boldsymbol{r}_{m_r} \end{bmatrix} \tag{B.1}$$

contains all m_r physical rigid body modes $\boldsymbol{r}_j$ of the linear system of Eq. (1)

$$\boldsymbol{M} \ddot{\boldsymbol{u}} + \boldsymbol{C} \dot{\boldsymbol{u}} + \boldsymbol{K} \boldsymbol{u} = \boldsymbol{f}, \tag{1}$$

which fulfill

$$\boldsymbol{K} \boldsymbol{r}_j = \boldsymbol{0} \quad \text{for} \quad j = 1, \ldots, m_r \quad \Leftrightarrow \quad \boldsymbol{K} \boldsymbol{R} = \boldsymbol{0}. \tag{B.2}$$

Each physical rigid body mode $\boldsymbol{r}_j$ can also be seen as eigenvector of eigenproblem Eq. (2)

$$\left(-\omega_j^2 \boldsymbol{M} + \boldsymbol{K} \right) \boldsymbol{\theta}_j = \boldsymbol{0} \tag{2}$$

---

[2]The standard eigenvalue problem Eq. (A.1) is obtained with $\boldsymbol{D} = -\boldsymbol{A}^{-1} \boldsymbol{B}$ if matrix $\boldsymbol{A}$ is invertible.

corresponding to eigenvalue $\omega_j^2 = 0$. For each physical rigid body mode $\boldsymbol{r}_j$ (or in other words: eigenvector $\boldsymbol{\theta}_j$ corresponding to eigenvalue $\omega_j^2 = 0$), there will be one or two eigenvalues $\sigma_j = 0$ if the corresponding state-space eigenproblem

$$(\sigma_j \boldsymbol{\mathcal{A}} + \boldsymbol{\mathcal{B}}) \, \boldsymbol{\theta}_{\mathrm{ss},j} = \boldsymbol{0} \tag{B.3}$$

is solved. For $\sigma_j = 0$, instead of Eq. (B.3), one can write

$$\boldsymbol{\mathcal{B}} \boldsymbol{\theta}_{\mathrm{ss},j} = \boldsymbol{0} \qquad \Leftrightarrow \qquad \begin{bmatrix} \boldsymbol{K} & \boldsymbol{0} \\ \boldsymbol{0} & -\boldsymbol{M} \end{bmatrix} \begin{bmatrix} \boldsymbol{\theta}_{\mathrm{ss},j,u} \\ \boldsymbol{\theta}_{\mathrm{ss},j,v} \end{bmatrix} = \begin{bmatrix} \boldsymbol{K} \boldsymbol{\theta}_{\mathrm{ss},j,u} \\ -\boldsymbol{M} \boldsymbol{\theta}_{\mathrm{ss},j,v} \end{bmatrix} = \begin{bmatrix} \boldsymbol{0} \\ \boldsymbol{0} \end{bmatrix}. \tag{B.4}$$

Thereby, $\boldsymbol{\theta}_{\mathrm{ss},j}$ is partitioned in displacement part $\boldsymbol{\theta}_{\mathrm{ss},j,u}$ and velocity part $\boldsymbol{\theta}_{\mathrm{ss},j,v}$. For positive definite mass matrix $\boldsymbol{M}$, the velocity part $\boldsymbol{\theta}_{\mathrm{ss},j,v}$ in Eq. (B.4) must be zero. The first row of Eq. (B.4) reproduces Eq. (B.2). This leads to the corresponding regular state-space rigid body mode

$$\boldsymbol{r}_{\mathrm{ss},j,\mathrm{reg}} = \begin{bmatrix} \boldsymbol{r}_j \\ \boldsymbol{0} \end{bmatrix} \tag{B.5}$$

There will be m_r such regular state-space rigid body modes $\boldsymbol{r}_{\mathrm{ss},j,\mathrm{reg}}$ and each of them has its physical corresponding part $\boldsymbol{r}_j$. Matrix $\boldsymbol{R}_{\mathrm{ss},\mathrm{reg}}$ contains all m_r regular state-space rigid body modes $\boldsymbol{r}_{\mathrm{ss},j,\mathrm{reg}}$ as columns:

$$\boldsymbol{R}_{\mathrm{ss},\mathrm{reg}} = \begin{bmatrix} \boldsymbol{r}_{\mathrm{ss},1,\mathrm{reg}} & \boldsymbol{r}_{\mathrm{ss},2,\mathrm{reg}} & \cdots & \boldsymbol{r}_{\mathrm{ss},m_r,\mathrm{reg}} \end{bmatrix} = \begin{bmatrix} \boldsymbol{R} \\ \boldsymbol{0} \end{bmatrix} \tag{B.6}$$

Matrix $\boldsymbol{R}$ contains the physical rigid body modes as columns as given by Eq. (B.1). As given by Eq. (B.5), each physical rigid body mode $\boldsymbol{r}_j$ has one corresponding regular state-space rigid body mode $\boldsymbol{r}_{\mathrm{ss},j,\mathrm{reg}}$. This relation is independent of the damping properties of the underlying system.

Appendix B.1. Undamped case

Consider the undamped equations of motion, i.e., Eq. (1) with $\boldsymbol{C} = \boldsymbol{0}$. The corresponding state-space eigenvalue problem is given by Eq. (B.3). For this case, each eigenvalue $\sigma_j = 0$ occurs as a root of multiplicity two [25, 38]. Thus, the eigenvalue problem is defective [6]. It possesses one set of n_r regular state-space rigid body modes $\boldsymbol{r}_{\mathrm{ss},j,\mathrm{reg}}$ given by Eq. (B.6). For each regular state-space rigid body mode $\boldsymbol{r}_{\mathrm{ss},j,\mathrm{reg}}$ corresponding to $\sigma_j = 0$, there is also a generalized state-space rigid body mode $\boldsymbol{r}_{\mathrm{ss},j,\mathrm{gen}}$, defined by Eq. (A.10):

$$\boldsymbol{\mathcal{A}} \begin{bmatrix} \boldsymbol{r}_{\mathrm{ss},j,\mathrm{reg}} & \boldsymbol{r}_{\mathrm{ss},j,\mathrm{gen}} \end{bmatrix} \begin{bmatrix} 0 & 1 \\ 0 & 0 \end{bmatrix} + \boldsymbol{\mathcal{B}} \begin{bmatrix} \boldsymbol{r}_{\mathrm{ss},j,\mathrm{reg}} & \boldsymbol{r}_{\mathrm{ss},j,\mathrm{gen}} \end{bmatrix} = \begin{bmatrix} \boldsymbol{0} & \boldsymbol{0} \end{bmatrix} \tag{B.7}$$

This gives two row partitions:

$$\boldsymbol{\mathcal{B}} \boldsymbol{r}_{\mathrm{ss},j,\mathrm{reg}} = \boldsymbol{0} \tag{B.8}$$

$$\boldsymbol{\mathcal{A}} \boldsymbol{r}_{\mathrm{ss},j,\mathrm{reg}} + \boldsymbol{\mathcal{B}} \boldsymbol{r}_{\mathrm{ss},j,\mathrm{gen}} = \boldsymbol{0} \tag{B.9}$$

Eq. (B.8) reproduces Eq. (B.4), which has already been used to determine the regular state-space rigid body mode $\boldsymbol{r}_{\mathrm{ss},j,\mathrm{reg}}$. Eq. (B.9) is now used to determine the generalized state-space rigid body mode $\boldsymbol{r}_{\mathrm{ss},j,\mathrm{gen}}$. With damping matrix $\boldsymbol{C} = \boldsymbol{0}$, matrix $\boldsymbol{\mathcal{A}}$ writes

$$\boldsymbol{\mathcal{A}} = \begin{bmatrix} \boldsymbol{0} & \boldsymbol{M} \\ \boldsymbol{M} & \boldsymbol{0} \end{bmatrix}. \tag{B.10}$$

Partitioning in displacement and velocity parts, Eq. (B.9) is

$$\begin{bmatrix} \boldsymbol{0} & \boldsymbol{M} \\ \boldsymbol{M} & \boldsymbol{0} \end{bmatrix} \begin{bmatrix} \boldsymbol{r}_{\mathrm{ss},j,\mathrm{reg},u} \\ \boldsymbol{r}_{\mathrm{ss},j,\mathrm{reg},v} \end{bmatrix} + \begin{bmatrix} \boldsymbol{K} & \boldsymbol{0} \\ \boldsymbol{0} & -\boldsymbol{M} \end{bmatrix} \begin{bmatrix} \boldsymbol{r}_{\mathrm{ss},j,\mathrm{gen},u} \\ \boldsymbol{r}_{\mathrm{ss},j,\mathrm{gen},v} \end{bmatrix} = \begin{bmatrix} \boldsymbol{0} \\ \boldsymbol{0} \end{bmatrix}, \tag{B.11}$$

which gives together with Eq. (B.5) the two row partitions:

$$M r_{\mathrm{ss},j,\mathrm{reg},v} + K r_{\mathrm{ss},j,\mathrm{gen},u} = \mathbf{0} \qquad \Rightarrow \qquad K r_{\mathrm{ss},j,\mathrm{gen},u} = \mathbf{0} \tag{B.12}$$

$$M r_{\mathrm{ss},j,\mathrm{reg},u} - M r_{\mathrm{ss},j,\mathrm{gen},v} = \mathbf{0} \qquad \Rightarrow \qquad M r_j - M r_{\mathrm{ss},j,\mathrm{gen},v} = \mathbf{0} \tag{B.13}$$

If M is nonsingular, Eq. (B.13) requires that

$$r_{\mathrm{ss},j,\mathrm{gen},v} = r_j. \tag{B.14}$$

Eq. (B.12) states either that $r_{\mathrm{ss},j,\mathrm{gen},u} = r_j$, i.e., the displacement part $r_{\mathrm{ss},j,\mathrm{gen},u}$ of $r_{\mathrm{ss},j,\mathrm{gen}}$ is equal to the physical rigid body mode or that $r_{\mathrm{ss},j,\mathrm{gen},u} = \mathbf{0}$ [6]. Since the regular state-space rigid body mode $r_{\mathrm{ss},j,\mathrm{reg}}$ already contains the physical rigid body mode r_j as displacement part $r_{\mathrm{ss},j,\mathrm{reg},u}$, it is sufficient to set $r_{\mathrm{ss},j,\mathrm{gen},u} = \mathbf{0}$ [6]. The generalized state-space rigid body mode $r_{\mathrm{ss},j,\mathrm{gen}}$ finally writes

$$r_{\mathrm{ss},j,\mathrm{gen}} = \begin{bmatrix} r_{\mathrm{ss},j,\mathrm{gen},u} \\ r_{\mathrm{ss},j,\mathrm{gen},v} \end{bmatrix} = \begin{bmatrix} \mathbf{0} \\ r_j \end{bmatrix}. \tag{B.15}$$

Thus, the complete set of $2m_r$ state-space rigid body modes for an undamped system is [6]

$$R_{\mathrm{ss}} = \begin{bmatrix} R_{\mathrm{ss},\mathrm{reg}} & R_{\mathrm{ss},\mathrm{gen}} \end{bmatrix} = \begin{bmatrix} R & \mathbf{0} \\ \mathbf{0} & R \end{bmatrix}. \tag{B.16}$$

As given by Eq. (B.5), each physical rigid body mode r_j has one corresponding regular state-space rigid body mode $r_{\mathrm{ss},j,\mathrm{reg}}$ independent of the damping properties of the underlying system. As given by Eq. (B.15), each physical rigid body mode r_j of an undamped system has additionally one corresponding generalized state-space rigid body mode $r_{\mathrm{ss},j,\mathrm{gen}}$. To sum up, as given by Eq. (B.16), each physical rigid body mode r_j of an undamped system has one corresponding regular state-space rigid body mode $r_{\mathrm{ss},j,\mathrm{reg}}$ and one corresponding generalized state-space rigid body mode $r_{\mathrm{ss},j,\mathrm{gen}}$.

Appendix B.2. Damped case

With damping matrix $C \neq \mathbf{0}$, matrix $\mathcal{A}$ writes

$$\mathcal{A} = \begin{bmatrix} C & M \\ M & \mathbf{0} \end{bmatrix} \tag{B.17}$$

and Eq. (B.11) changes to

$$\begin{bmatrix} C & M \\ M & \mathbf{0} \end{bmatrix} \begin{bmatrix} r_{\mathrm{ss},j,\mathrm{reg},u} \\ r_{\mathrm{ss},j,\mathrm{reg},v} \end{bmatrix} + \begin{bmatrix} K & \mathbf{0} \\ \mathbf{0} & -M \end{bmatrix} \begin{bmatrix} r_{\mathrm{ss},j,\mathrm{gen},u} \\ r_{\mathrm{ss},j,\mathrm{gen},v} \end{bmatrix} = \begin{bmatrix} \mathbf{0} \\ \mathbf{0} \end{bmatrix}, \tag{B.18}$$

which gives now together with Eq. (B.5) the following two row partitions:

$$C r_{\mathrm{ss},j,\mathrm{reg},u} + M r_{\mathrm{ss},j,\mathrm{reg},v} + K r_{\mathrm{ss},j,\mathrm{gen},u} = \mathbf{0} \qquad \Rightarrow \qquad C r_j + K r_{\mathrm{ss},j,\mathrm{gen},u} = \mathbf{0} \tag{B.19}$$

$$M r_{\mathrm{ss},j,\mathrm{reg},u} - M r_{\mathrm{ss},j,\mathrm{gen},v} = \mathbf{0} \qquad \Rightarrow \qquad M r_j - M r_{\mathrm{ss},j,\mathrm{gen},v} = \mathbf{0} \tag{B.20}$$

Eq. (B.20) reproduces Eq. (B.13), which requires that $r_{\mathrm{ss},j,\mathrm{gen},v} = r_j$ (as for the undamped case). Eq. (B.12) has now changed to Eq. (B.19). Keep in mind that K is singular and consider Eq. (B.19):

- If $C r_j = \mathbf{0}$, solving Eq. (B.19) is equal to the solution of the undamped case. A solution for $r_{\mathrm{ss},j,\mathrm{gen},u}$ exists and the generalized state-space rigid body mode $r_{\mathrm{ss},j,\mathrm{gen}}$ is given by Eq. (B.15).

- If $C r_j \neq \mathbf{0}$, Eq. (B.19) does not have a solution since K is singular. The assumption that $\sigma_j = 0$ has multiplicity two, leading to a regular and a generalized state-space rigid body mode, is not valid [6]. Only a regular state-space rigid body mode $r_{\mathrm{ss},j,\mathrm{reg}}$ exists and no corresponding generalized state-space rigid body $r_{\mathrm{ss},j,\mathrm{gen}}$ mode occurs.

23

Therefore, the result of $\boldsymbol{Cr}_j$ is used as indicator for the occurrence of generalized state-space rigid body modes $\boldsymbol{r}_{\mathrm{ss},j,\mathrm{gen}}$ for damped systems. As described before, each physical rigid body mode $\boldsymbol{r}_j$ has one corresponding regular state-space rigid body mode $\boldsymbol{r}_{\mathrm{ss},j,\mathrm{reg}}$. Each physical rigid body mode $\boldsymbol{r}_j$ of an undamped system has also one corresponding generalized state-space rigid body mode $\boldsymbol{r}_{\mathrm{ss},j,\mathrm{gen}}$. Each physical rigid body mode $\boldsymbol{r}_j$ of a damped system can have one corresponding generalized state-space rigid body mode $\boldsymbol{r}_{\mathrm{ss},j,\mathrm{gen}}$, but does not have to have one. The existence of the generalized state-space rigid body mode $\boldsymbol{r}_{\mathrm{ss},j,\mathrm{gen}}$ depends on the structure of the damping matrix $\boldsymbol{C}$. The criterion $\boldsymbol{Cr}_j$ is used to detect if a physical rigid body mode $\boldsymbol{r}_j$ of a damped system does have one corresponding generalized state-space rigid body mode $\boldsymbol{r}_{\mathrm{ss},j,\mathrm{gen}}$ or does not.

References

[1] R. R. Craig, M. C. C. Bampton, Coupling of Substructures for Dynamic Analyses, AIAA Journal 6 (7) (1968) 1313–1319. doi:10.2514/3.4741.
URL http://dx.doi.org/10.2514/3.4741

[2] R. H. MacNeal, A hybrid method of component mode synthesis, Computers and Structures 1 (4) (1971) 581–601. doi:10.1016/0045-7949(71)90031-9.

[3] S. Rubin, Improved Component-Mode Representation for Structural Dynamic Analysis, AIAA Journal 13 (8) (1975) 995–1006. doi:10.2514/3.60497.
URL http://arc.aiaa.org/doi/abs/10.2514/3.60497

[4] R. R. Craig, Coupling of substructures for dynamic analyses: An overview, in: Proceedings of AIAA/ASME/ASCE/AHS/ASC structures, structural dynamics, and materials conference and exhibit, Atlanta, GA, USA, 2000, pp. 1573–1584.

[5] D. J. Rixen, A dual Craig-Bampton method for dynamic substructuring, Journal of Computational and Applied Mathematics 168 (1-2) (2004) 383–391. doi:10.1016/j.cam.2003.12.014.

[6] R. R. Craig, A. J. Kurdila, Fundamentals of structural dynamics, John Wiley & Sons, 2006.

[7] S. N. Voormeeren, P. L. C. Van Der Valk, D. J. Rixen, Generalized Methodology for Assembly and Reduction of Component Models for Dynamic Substructuring, AIAA Journal 49 (5) (2011) 1010–1020. doi:10.2514/1.J050724.
URL http://arc.aiaa.org/doi/abs/10.2514/1.J050724http://arc.aiaa.org/doi/10.2514/1.J050724

[8] F. M. Gruber, D. J. Rixen, Evaluation of Substructure Reduction Techniques with Fixed and Free Interfaces, Strojniški vestnik - Journal of Mechanical Engineering 62 (7-8) (2016) 452–462. doi:10.5545/sv-jme.2016.3735.
URL http://ojs.sv-jme.eu/index.php/sv-jme/article/view/sv-jme.2016.3735

[9] R. R. Craig, C.-J. Chang, On the use of attachment modes in substructure coupling for dynamic analysis, in: 18th Structural Dynamics and Materials Conference, Structures, Structural Dynamics, and Materials and Co-located Conferences, American Institute of Aeronautics and Astronautics, San Diego, CA, USA, 1977, pp. 89–99. doi:10.2514/6.1977-405.
URL http://dx.doi.org/10.2514/6.1977-405

[10] D. N. Herting, A general purpose, multi-stage, component modal synthesis method, Finite elements in analysis and design 1 (2) (1985) 153–164.

[11] K. C. Park, Y. H. Park, Partitioned Component Mode Synthesis via a Flexibility Approach, AIAA Journal 42 (6) (2004) 1236–1245. doi:10.2514/1.10423.
URL https://doi.org/10.2514/1.10423

[12] R. R. Craig, Y.-T. Chung, A generalized substructure coupling procedure for damped systems, in: 22nd Structures, Structural Dynamics and Materials Conference, Structures, Structural Dynamics, and Materials and Co-located Conferences, American Institute of Aeronautics and Astronautics, Atlanta, GA, USA, 1981, pp. 254–266. doi:10.2514/6.1981-560.
URL http://dx.doi.org/10.2514/6.1981-560

[13] T. K. Hasselman, Damping Synthesis from Substructure Tests, AIAA Journal 14 (10) (1976) 1409–1418. doi:10.2514/3.61481.
URL http://arc.aiaa.org/doi/abs/10.2514/3.61481

[14] Y.-T. Chung, R. R. Craig, State vector formulation of substructure coupling for damped systems, in: Proc. of the 24th AIAA/ASME/ASCE/AHS Structures, Structural Dynamics and Materials Conf, 1983, pp. 520–528.

[15] R. R. Craig, Y.-T. Chung, Generalized substructure coupling procedure for damped systems, AIAA journal 20 (3) (1982) 442–444. doi:10.2514/3.51089.
URL https://arc.aiaa.org/doi/abs/10.2514/3.51089

[16] J.-G. Beliveau, Y. Soucy, Damping synthesis using complex substructure modes and a Hermitian system representation, AIAA Journal 23 (12) (1985) 1952–1956. doi:10.2514/3.9201.
URL http://dx.doi.org/10.2514/3.9201

[17] T. K. Caughey, Classical Normal Modes in Damped Linear Dynamic Systems, Journal of Applied Mechanics 27 (2) (1960) 269–271. doi:10.1115/1.3643949.
URL http://dx.doi.org/10.1115/1.3643949

[18] R. A. Frazer, W. J. Duncan, A. R. Collar, Elementary matrices and some applications to dynamics and differential equations, Cambridge University Press, 1938.

[19] W. C. Hurty, M. F. Rubinstein, Dynamics of structures, Prentice-Hall, Inc., Englewood Cliffs, New Jersey, USA, 1964.

[20] T. K. Hasselman, A. Kaplan, Dynamic Analysis of Large Systems by Complex Mode Synthesis, Journal of Dynamic Systems, Measurement, and Control 96 (3) (1974) 327–333. `doi:10.1115/1.3426810`.
URL `http://dx.doi.org/10.1115/1.3426810`

[21] T. G. Howsman, R. R. Craig, A substructure coupling procedure applicable to general linear time-invariant dynamic systems, in: 25th Structures, Structural Dynamics and Materials Conference, Structures, Structural Dynamics, and Materials and Co-located Conferences, American Institute of Aeronautics and Astronautics, Reston, Virigina, 1984, pp. 164–171. `doi:10.2514/6.1984-944`.
URL `http://arc.aiaa.org/doi/10.2514/6.1984-944`

[22] R. R. Craig, Z. Ni, Component mode synthesis for model order reduction of nonclassicallydamped systems, Journal of Guidance, Control, and Dynamics 12 (4) (1989) 577–584. `doi:10.2514/3.20446`.
URL `http://dx.doi.org/10.2514/3.20446`

[23] E. Brechlin, L. Gaul, Two methodological improvements for component mode synthesis, in: PROCEEDINGS OF THE INTERNATIONAL SEMINAR ON MODAL ANALYSIS, Vol. 3, KU Leuven, 2001, pp. 1127–1134.

[24] A. de Kraker, Generalization of the Craig-Bampton CMS procedure for general damping, Tech. rep., Technische Universiteit Eindhoven, Vakgroep Fundamentele Werktuigkunde, Rapportnr. WFW 93.023 (1993).

[25] A. de Kraker, D. H. van Campen, Rubin's CMS reduction method for general state-space models, Computers & Structures 58 (3) (1996) 597–606. `doi:10.1016/0045-7949(95)00151-6`.
URL `https://doi.org/10.1016/0045-7949(95)00151-6`

[26] D. J. Rixen, Dual Craig-Bampton with enrichment to avoid spurious modes, Proceedings of IMAC-XXVII.

[27] J.-H. Kim, J. Kim, P.-S. Lee, Improving the accuracy of the dual Craig-Bampton method, Computers & Structures 191 (2017) 22–32. `doi:10.1016/j.compstruc.2017.05.010`.
URL `http://www.sciencedirect.com/science/article/pii/S0045794917300846`

[28] F. Ma, A. Imam, M. Morzfeld, The decoupling of damped linear systems in oscillatory free vibration, Journal of Sound and Vibration 324 (1) (2009) 408–428. `doi:10.1016/j.jsv.2009.02.005`.
URL `https://doi.org/10.1016/j.jsv.2009.02.005`

[29] T. K. Caughey, M. E. J. O'Kelly, Classical Normal Modes in Damped Linear Dynamic Systems, Journal of Applied Mechanics 32 (3) (1965) 583–588. `doi:10.1115/1.3627262`.
URL `http://dx.doi.org/10.1115/1.3627262`

[30] J. W. S. B. Rayleigh, The Theory of Sound, Vol. 2, Macmillan, 1896.

[31] G. F. Lang, Understanding Modal Vectors, Springer International Publishing, Cham, 2017, pp. 55–68. `doi:10.1007/978-3-319-54810-4_8`.
URL `http://dx.doi.org/10.1007/978-3-319-54810-4{_}8`

[32] E. Balmès, New results on the identification of normal modes from experimental complex modes, Mechanical Systems and Signal Processing 11 (2) (1997) 229–243. `doi:10.1006/MSSP.1996.0058`.
URL `http://www.sciencedirect.com.ezproxy.library.wisc.edu/science/article/pii/S0888327096900588`

[33] C. Farhat, M. Geradin, On a component mode synthesis method and its application to incompatible substructures, Computers & Structures 51 (5) (1994) 459–473. `doi:10.1016/0045-7949(94)90053-1`.
URL `https://www.sciencedirect.com/science/article/pii/0045794994900531`

[34] J. C. Simo, P. Wriggers, R. L. Taylor, A perturbed Lagrangian formulation for the finite element solution of contact problems, Computer Methods in Applied Mechanics and Engineering 50 (2) (1985) 163–180. `doi:https://doi.org/10.1016/0045-7825(85)90088-X`.
URL `http://www.sciencedirect.com/science/article/pii/004578258590088X`

[35] C. Bernardi, N. Debit, Y. Maday, Coupling finite element and spectral methods: First results, Mathematics of Computation 54 (189) (1990) 21–39.

[36] D. D. Klerk, D. J. Rixen, S. N. Voormeeren, General Framework for Dynamic Substructuring: History, Review and Classification of Techniques, AIAA Journal 46 (5) (2008) 1169–1181. `doi:10.2514/1.33274`.

[37] M. Géradin, D. J. Rixen, Mechanical vibrations: theory and application to structural dynamics, John Wiley & Sons, 2015.

[38] R. R. Craig, T.-J. Su, Z. Ni, State-variable models of structures having rigid-body modes, Journal of Guidance, Control, and Dynamics 13 (6) (1990) 1157–1160. `doi:10.2514/3.20594`.
URL `http://dx.doi.org/10.2514/3.20594`

[39] A. de Kraker, The RUBIN CMS procedure for general state-space models, Tech. rep., Technische Universiteit Eindhoven, Vakgroep Fundamentele Werktuigkunde, Rapportnr. Rapportnr. WFW 94.081 (1994).

[40] R. J. Allemang, D. L. Brown, A correlation coefficient for modal vector analysis, in: Proceedings of the 1st international modal analysis conference, Vol. 1, Orlando, 1982, pp. 110–116.

[41] R. J. Allemang, The modal assurance criteriontwenty years of use and abuse, Sound and vibration 37 (8) (2003) 14–23.

[42] D. J. Rixen, Interface Reduction in the Dual Craig-Bampton method based on dual interface modes, Springer New York, New York, NY, 2011, pp. 311–328. `doi:10.1007/978-1-4419-9305-2_22`.
URL `http://dx.doi.org/10.1007/978-1-4419-9305-2{_}22`

[43] F. M. Gruber, M. Gille, D. J. Rixen, Time integration of dual Craig-Bampton reduced systems, in: Proceedings of COMPDYN 2017, 6th International Conference on Computational Methods in Structural Dynamics and Earthquake Engineering, 2017.

[44] C.-T. Chen, Linear system theory and design, 2nd Edition, Oxford University Press, Inc., New York, NY, USA, 1995.

[45] G. H. Golub, C. F. Van Loan, Matrix computations, Vol. 4, The Johns Hopkins University Press, Baltimore, 2013.